INVESTIGATION ON ELECTRICAL PROPERTIES, MORPHOLOGICAL ANALYSIS AND SURFACE ROUGHNESS OF SILVER NANOPARTICLES-FILLED EPOXY CONDUCTIVE INK

ROSHIDAH BINTI HAMIDI

UNIVERSITI TEKNIKAL MALAYSIA MELAKA

SUPERVISOR'S DECLARATION

I hereby declare that I have read this project and in my opinion this report is sufficient in terms of scope and quality for the award of the degree of Bachelor of Mechanical Engineering.

Signature	:……..
Supervisor's name	:……..
Date	:……..

INVESTIGATION ON ELECTRICAL PROPERTIES, MORPHOLOGICAL ANALYSIS AND SURFACE ROUGHNESS OF SILVER NANOPARTICLES-FILLED EPOXY CONDUCTIVE INK

ROSHIDAH BINTI HAMIDI

A report submitted
in fulfilment of the requirements for
the degree of Bachelor of Mechanical Engineering

Faculty of Mechanical Engineering

UNIVERSITI TEKNIKAL MALAYSIA MELAKA

2018

PENYIASATAN PADA SIFAT-SIFAT ELEKTRIKAL, ANALISIS MORFOLOGI DAN KEKASARAN PERMUKAAN DAKWAT KONDUKTIF NANOPARTIKEL PERAK YANG MENGANDUNGI EPOKSI

ROSHIDAH BINTI HAMIDI

Laporan ini dikemukakan sebagai
memenuhi sebahagian daripada syarat penganugerahan
Ijazah Sarjana Muda Kejuruteraan Mekanikal

Fakulti Kejuruteraan Mekanikal

UNIVERSITI TEKNIKAL MALAYSIA MELAKA

2018

DECLARATION

I declare that this project entitled "Investigation on Electrical Properties, Morphological Analysis and Surface Roughness of Silver Nanoparticles-filled Epoxy Conductive Ink" is the result of my own work except as cited in the references.

Signature :…….

Name :…….

Date :…….

DEDICATION

To my beloved mother, Rohani binti Ismail and
late father, Hamidi bin Mohd Nor

ABSTRACT

This study aspires to have an analysis of silver nanoparticles-filled epoxy conductive ink. Specifically, the parameters that were evaluated consist of sheet resistivity, surface texture and morphological analysis. In order to accomplish the analysis, four point probe is used to measure the sheet resistance value of the sample in ohms-per-square. Some of percentage of ink loading has detected the presence of resistivity and some percentage has not detected any presence of resistivity. The highest average resistivity is detected in low percentage of ink loading while the lowest one is found in high percentage of ink loading. In terms of surface texture, contact profilometer was used which resulted that the samples with lower filler percentage had consistent average value of surface roughness and smooth surface. Meanwhile, for the samples with high percentage of filler had inconsistent surface irregularities that contributed to rougher surface. In morphological analysis, light microscope is used to visualize the microscopic image of silver nanoparticles ink categorized by the electrical properties of the ink. Ink loading with high percentage of silver nanoparticles has conductivity while low percentage has no conductivity. At low percentage, the microstructure image shows no appearance of silver nanoparticles element while for high percentage; the image shows the content of filler loading. The future researchers can use different type of substrate or different materials of conductive ink in order to do the same analysis.

ABSTRAK

Kajian ini bercita-cita untuk menganalisis dakwat konduktif nanopartikel perak yang ,mengandungi epoksi. Secara khususnya, parameter yang dinilai terdiri daripada resistiviti lembaran, tekstur permukaan dan analisis morfologi. Untuk mencapai analisis, prob empat titik digunakan untuk mengukur nilai rintangan lembaran sampel dalam ohms-per-kuadrat. Beberapa peratusan kandungan dakwat telah mengesan kehadiran resistiviti dan beberapa peratusan lagi tidak mengesan kehadiran resistivitas. Purata resistiviti tertinggi dikesan dalam kandungan dakwat yang berperatusan rendah manakala resistiviti yang paling rendah didapati dalam kandungan dakwat yang berperatusan tinggi. Dari segi tekstur permukaan, profilometer sentuh digunakan di mana sampel yang mengandungi peratusan pengisi rendah mempunyai purata nilai kekasaran permukaan yang konsisten dan permukaan yang licin dihasilkan. Sementara itu, bagi sampel yang mengandungi peratusan pengisi tinggi, ia mempunyai kekasaran permukaan yang tidak konsisten lalu menyumbang kepada permukaan yang lebih kasar. Dalam analisis morfologi, mikroskop cahaya digunakan untuk memvisualisasikan imej mikroskopik dakwat nanopartikel perak yang dikategorikan oleh sifat-sifat elektrik dakwat. Kandungan dakwat dengan peratusan nanopartikel perak yang tinggi mempunyai kekonduksian manakala dakwat yang berperatusan rendah tidak mempunyai kekonduksian. Pada peratusan rendah, imej mikrostruktur tidak memperlihatkan unsur nanopartikel perak manakala peratusan yang tinggi; imej menunjukkan kandungan pengisi. Penyelidik masa depan boleh menggunakan jenis substrat yang berlainan atau bahan berlainan dalam dakwat konduktif untuk melakukan analisis yang sama.

ACKNOWLEDGEMENTS

Thanks to Allah Almighty as with His Bestowment and His Mercy, I have completely succeeded this project. I revere the patronage and moral support extended with love, by my mother whose financial support and passionate encouragement made it possible for me to complete this project and not to forget my late father who is always in my prayers.

I want to express my heartiest gratitude to my supervisor, Dr. Mohd Azli bin Salim for his sincere guidance, support and help me with a lot of patience as well as provide me with valuable knowledge throughout the whole duration in completing this project.

I am deeply indebted to all concerned persons who cooperated with me in this regard for their valuable help in preparing this project. My joy knows no bounds in expressing my cordial gratitude to my friends as their keen interest and encouragement were a great help throughout the course of this project.

I humbly extend my thanks to all people that involved either directly or indirectly in order to complete this project

TABLE OF CONTENTS

LIST OF TABLES

LIST OF FIGURES

LIST OF ABBREVIATIONS

ρ	-	Resistivity
A	-	Cross-sectional area of the ink
L	-	Length of sample trace from end to end
R	-	Resistance
l	-	Length of line in mm
W	-	Width in mm
R_{SH}	-	Resistivity of the sheet in *Ohm/sq, Ω/sq*
V	-	Voltage across the inner pins
I	-	Current between the outer pins
T_m	-	Melting point
E	-	Estimation of error
Ra	-	Average of roughness

CHAPTER 1

INTRODUCTION

1.1 BACKGROUND OF STUDY

Conductive ink, ink printed to conduct electricity have been in some talk for a few years for their applications in Printed Electronics (PE) and Flexible Electronics (FE) as people will be able to print circuits on paper or some form of flexible surface through the inkjet printing technology. Although the early growth of the printed electronics industry is not drastic compared to the expected growth, due to high expectation, there are some great demands to use these products (conductive inks) in daily activities such as cell phones, displays, smart wearable, lighting, small packaging, labels, shipping, storage or any else.

Figure 1.1 Printed conductive ink (Savastano, "Conductive Inks Drive Growth in Flexible and Printed Electronics ", 2015)

Conductive ink has allowed some improvements in the electronics sector, thus enable the disposable electronics to develop in real world. Some factors such as good production performances, followed by reductions of material cost as well as environmental-wise (due to non-etching manufacturing procedures) lead to the

alternative yet efficient way for end-use applications via conductive inks through PE and FE.

Material selection is one of critical success to take into consideration in formulating the conductive ink. Basically conductive ink consists of two main components; metal nanoparticles (usually silver), and liquid to carry the nanoparticles. When the mixture of both nanoparticles and liquid is printed to paper, it will dry, and the random connections of nanoparticles creating bridge to each other are put in place.

Electrical conduction is the electron movement via a material, providing an electric current. Conductive components are part of conductive ink that may consist of silver, carbon, graphite, or other precious metal coated base material. Some materials can naturally enable the electrons to travel through them, and they are known as electrical conductors. Metals are usually specialized in best conducting the electricity, but, in order to produce conductive ink, a liquid is needed, and most metals are in solid state at room temperature.

In other ways to produce conductive ink but still using metals, metal nanoparticles are chosen to realize it. These nanoparticles are in the form of tiny spheres of metal, where each of nanoparticles can conduct electricity, and when the strings of nanoparticles; pearls-in-a-necklace-like-chain are formed, electrons can flow from one nanoparticle to another.

In this study, silver nanoparticles are part of components in conductive ink that act as a filler material. Filler is used to fill the unfilled space between the particles which may lead to form conductive coating as silver is one of the best electric conductor.

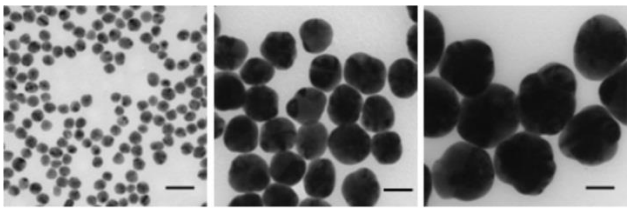

Figure 1.2 Transmission electron microscopy (TEM) images of silver nanoparticles (Oldenburg, "Silver Nanoparticles: Properties and Applications", 2017)

As for the liquid to carry the nanoparticles, there are two types of liquid with different viscosity, functioned as the binder and the hardener. Epoxy used as binder in this study is compatible to the viscosity behaviours of inks. It shows the anticorrosion properties when acting as coating ingredients. While for the hardener, it is an additional substance to the ink mixture to produce the ink finish strong or more durable, as well as the curing agent for epoxy. The final result of mixture from these three components is a conductive ink that maintains in liquid form until printed on certain surface at its drying point and succeed to conduct electricity.

In this study, troubleshooting problems in the characterization of conductive ink are elucidated to fabricate conductive ink which has high conductivity tracks or patterns. The characterization of conductive may consist of the parameters involved, the formulation of ink loading, the printing procedure, ink-substrate interaction, the temperature to cure and post-treatment of inks.

For the formulation of ink loading, the interaction between filler, binder and hardener is important as it is the preliminary step to find out which ink loading can be resulted to have high conductivity. The ink loading is printed on the glass substrate, and then they will go through preheating method where the ink loading is cured in the oven for specialized time and temperature. The characterization of conductive ink is investigated so that a proper understanding may be gained through various methods (analysis); four point probe for sheet resistivity, contact profilometer for surface texture and light microscope for morphological analysis.

All these described steps are repeated for the ink loading in accordance to the composition of element to produce conductive ink. This study highlights two research questions about the formulation of silver nanoparticles-filled epoxy to produce conductive ink and the relationship between all of the parameters investigated for silver nanoparticles-filled epoxy.

1.2 PROBLEM STATEMENT

The method of fabricating electrical circuits using conductive ink will take the place of the current method of creating circuit boards. The conductive ink depends on the formation ways of metal nanoparticles, thus the issues that need attention are the materials composition and its behaviour to have high conductivity ink as the drawback to conductive ink circuits is their resistance.

Choosing the right ink loading is a crucial success factor for quick, simple and affordable production of PE prototypes and electronically functional prints. One of the issues where the ink loading needs alteration is when the conductive inks are not fully dried after curing at certain temperature. Another issue is the ink-substrate interaction; the ink easily comes off of the substrate after printing or curing process which indicates that a compatibility issue may come in between the ink and substrate, or the ink may not be dried adequately.

Recently, most researchers around the world studied the effect of conductive ink for silver nanoparticles-filled epoxy by implementing measurement techniques to conductive ink in order to maximize the quality and reliability of conductive ink through three techniques (Samano, A., 2017). In this report, the measurements involved are sheet resistivity, surface texture and morphological behaviour for sheet resistivity; Samano described that four point probe measures the sample with no error produced by test lead resistance. Next, for the surface roughness, it is one of the main contributors that affect the electrical resistivity of printings on the substrate (Maattanen, A et al., 2010) and imaging methods from conventional microscope can contribute image with fine details that included elemental details of printed sample (Ikeda, O., Watanabe, Y., & Itoh, F., 2007).

After all, all of the issues of the conductive ink stated are linked to the formulation of ink loading, not being mentioned, another additional factors such as material selection, printing method, curing temperature and others. Therefore, the purpose of this study may come out with the solutions for the problems stated.

1.3 OBJECTIVES

The objectives of this study are:

1. To formulate silver nanoparticles-filled epoxy for conductive ink.
2. To investigate the relationship for silver nanoparticles-filled epoxy between sheet resistivity, surface texture and morphological analysis.

1.4 SCOPE OF PROJECT

In order to reach the objectives, several scopes have been decided:

1. Formulating silver nanoparticles for patterning conductive ink which consists of filler (silver nanoparticles), binder (epoxy) and hardener.
2. Evaluating the effect of silver nanoparticles conductive ink in constant temperature by using 4-point probe, microscope and contact profilometer.

1.5 HYPOTHESIS

From this study, the expected result is the optimum parameter will be obtained to improve the conductive ink by formulating the ink loading between filler and binder. The result should be found in the best conductivity of the ink in various patterns at constant temperature to cure.

1.6 REPORT OUTLINE

The structure of this report consists of five chapters. In Chapter 2, all of the related information from the literature review collection will be presented so that the comparison between the previous research, current and expected research can be made in order to ensure there is no similar research about this project has been made.

From Chapter 3, the research methodology will be displayed by stating the steps or procedures taken in the experiment based on the flowchart constructed. This chapter will present from the beginning of the experiment until the testing process; electrical testing, microscopy and surface roughness measurement so that the analysis can be made.

Then, in Chapter 4, when the results from the previous chapter has been obtained, the analysis will be discussed in this chapter in terms of the behaviour of the ink; mainly resistivity, and microstructure plus the surface roughness in order to answer the questions in this research.

Lastly, after the analysis has been carried out, only then the conclusion of this experiment will be revealed in Chapter 5; whether the objectives have been achieved or not.

CHAPTER 2

LITERATURE REVIEW

2.1 INTRODUCTION

In this chapter, a review on conductive ink, methods of printing, heat treatment, material of substrates and the conductive ink characterization are being presented with the sources from previous studies in this field.

2.2 CONDUCTIVE INK

According to Bhore, inks are specially fabricated in accordance to the demand of a printing process. In 2006, Karwa, A. stated that the conductive inks are made of the composition of a filler with resin, solvents and additives; where the fillers are responsible for providing the conductive properties, while the binder is needed to produce the required adhesion to the substrate and cohesion to each other. The conductivity of an ink is affected by the filler loading amount, the particle size of the fillers, the percentage of binder used and the continuity of the printed layer after the processes of printing and drying (Joshi, S. S., 2011).

2.2.1 Metal-based materials

According to Nir, M. M., Zamir, et al., the basic specification for metal-based inks is that they should present good electrical conductivity of the printed pattern as well as the ink should show great resolution and printability with least printer maintenance and show that the ink is compatible with the substrate. Furthermore, Kamyshny, A. et al. added that the ink should be processable in the means of annealing or curing temperatures below 150 °C, or better 120 °C to be comparable with that of flexible substrates such as polyethylene terephthalate (PET).

2.2.1.1 Silver

In 2013, Bhore described that the conductivity of printed silver layer is affected by the size and the shape of the particles. In terms of the shape, there are two types of silver ink; nano silver inks and silver flake inks. As claimed by Joshi in year 2011, the silver flakes are dried by the process of heating at temperatures and curing time; same goes to the nano silver inks by removing the solvent and leaving the binder and a film of conducting material on the substrate.

According to Nir, M. M., Zamir, et al., modification of the silver nanoparticles synthesis (in terms of particle size, stabilization) is one of necessary points in producing inks with high conductivity printed patterns thus, it demands of highly concentrated dispersions of loadings of silver nanoparticles, usually 20-40 $wt\%$. The $wt\%$ was obtained when the mass of silver nanoparticles were divided by the sum of weight of each ink, thus, for the $wt\%$, it consisted of the masses of the silver content and the masses of the capping agent (Shen et al., 2014).

In the description by Kim et al., the sintering process of silver nanoparticles can be resulted in high conductivity when a 20 nm diameter of silver nanoparticles are used and cured at range of temperatures of 100 – 300 °C for 30 min. The nanoparticles ink are sintered and often demands of temperatures ranged from 100 $°C$ until 400 °C and time to cure from 5 to 60 min, which is in accordance to the temperature (Joshi, S. S., 2011).

2.2.1.2 Copper

In 2013, Lupo et al. reported that copper has conductivity comparable to that of silver but a lot cheaper (approximately 5 €/kg in January 2014). Copper can be a good choice of material as mentioned by Park et al. in 2007 due to its less electromigration and lower cost than novel metals, but it is rapidly oxidized in the air which may worsen the conductivity.

Oxides are not conductive that causes the limitation in usage of copper in printed electronics applications. The usage of protecting agents for instance, ligands can shield copper in formulation of ink (Lupo et al., 2013). Otherwise, Kela, L. reminded that if not being protected in the application, it is limited to only several short lifespan products.

2.2.2 Carbon-based materials

Referring to (Kirkor et al., 2006; Joshi, S. S., 2011) carbon based inks contains some particles such as fullerene, amorphous carbon or graphite; where for graphite, it is the carbon formation that contains number of layers of graphene defined as a single sheet of carbon atoms.

Kirkor et al. also told that these inks are let to dry after being applied on the substrates; by using heat treatment in the range of 50 °C until to a several hundred degree Celsius which is essential to obtain high electrical conductivity. Bernds, A. et al., added that graphite is preferred to be in micro-platelets formation for printed electronics in order to attain good processability and electrical performance.

2.2.3 Carbon nanotube (CNT)

In 2007, Gruner, G. reported that CNT are better conductors than majority of polymers and display conductivity close to that of copper, they withstand tear and wear and they are chemically stable as they do not respond with majority of the chemicals, thus they are being applied in touch screens, solar cells, sensors and other devices

But, they are likely to agglomerate and do not create very stable dispersions; which affecting the electrical properties and for that reason, before carbon nanotube inks being printed, efficient techniques of dispersion need to be employed (Denneulin, A. et al., 2009).

2.2.4 Polymer

In 2015, Chen et al. reported that conductive polymers have been widely applied in various electronic devices such as light emitting displays and batteries. In regards of their organic nature, the adhesion between conductive polymer thin films and flexible plastic substrates and their mechanical stability are the best, mainly under bending conditions.

Among conductive polymers, poly(3,4-ethylenedioxythiophene) or PEDOT is considered as one of the most favourable technologically electrically conductive polymers as it has stable electrical conductivity and versatile processability.

2.2.5 Nanoparticles materials

For the purpose of this chapter, only silver nanoparticles material is the subject being highlighted. (Joshi, S. S., 2011; Burton, J., 2008) described that silver maintains its reputation as the first option of end-users despite the fact that it is the most high-priced material in-use; due to the benefits of its high conductivity, even when oxidized as well as it can be simply formulated into inks and its adhesive properties toward substrate is better than nickel and copper.

In terms of printing conditions, those inks should have a high amount of silver and require low 150 °C temperature of sintering yet silver metallic nanoparticles the most widely used as conductive fillers for ink-jet printing application (Moscicki, A. et al., 2005).

Allen, M. L. et al. stated that the printed patterns of nanoparticles inks mostly have high resistivity and needs a process of sintering at elevated temperatures (100 – 200 °C at 30 – 60 minutes) to distinguish stabilizers and/or some electrically non-conductive organic components to improve conductivity.

In 2015, Chen et al. tabulated the benefits and drawbacks of nanoparticle inks compared to other inks are listed in the table below.

Table 2.1 Metallic track comparison

	Sintering Temperature	Thickness Control	Ink Stability (Clogging)	Solvent Composition
Nanoparticle Inks	> 150 °C	Deposition layers	Poor	Multiple
MOD Inks	70 ~ 130 °C	Deposition layers	Good	Binary
Catalyst Inks	25 ~ 100 °C	Reaction times	Excellent	Single
Reaction Inkjet System	Room temperature	Reaction concentration	Excellent	Single

2.3 METHODS OF PRINTING

According to Krebs, F. C. in 2009, to achieve the required patterns, the inks can be put on various substrates using different coating methods or printing. The coating methods are defined as the layer of ink is shifted to the substrate by casting, spraying, pouring or smearing it over the surface of the substrate, while for printing, the layer of ink is shifted to a substrate from a stamp by an action of reversing.

In 2015, there are three techniques of depositing the ink tracks from Nash et al.; ink-jet printing, printing method and coating method. Krebs, F. C. added that ink-jet printing is a new method that can be put in both methods; printing and coating as it is possible to recreate a complex design in a single-step procedure.

There are some methods of depositing the ink tracks; casting, doctor-blading, flexographic and ink-jet printing as can be seen in figure below (Nash et al., 2015).

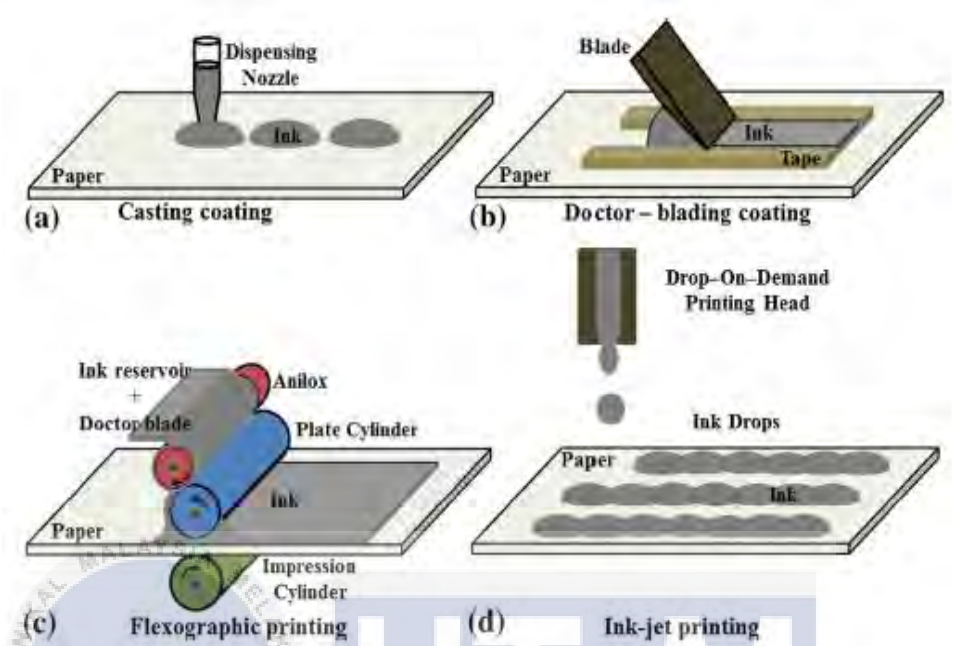

Figure 2.1 Some methods of depositing the ink tracks (Nash et al., 2015)

2.3.1 Casting coating

In casting method, there is no advanced equipment is required but a well horizontality of the surface of substrate is crucial to have. The ink is casted onto the substrate in two forms; liquid portion or isolated drops and then, the ink is being dried at elevated or room temperature. This method is allowed to obtain thick films with nice coating quality, but the accuracy of the film thickness control is what it lacks of (Nash et al., 2015).

2.3.2 Flexographic

Bois, C. et al. mentioned in 2012 that in flexographic method, it consists of transferring the required image using relief plates that enforce a low pressure onto the substrate. During the printing process, the ink is shifted to an anilox (micro-engraved cylinder) that are contained with a permanent volume of ink from a reservoir by using a doctor blade and then onto a printing plate (Nash et al., 2015).

According to Nash et al., while the inked pattern is compressed to the substrate between the printing cylinder and the printing plate, the ink film scission produced the ink transfer. When the printing of a solid pattern is done, its thickness is affected by on the number of ink layers, on the affinity of ink-substrate and the volume of ink in the anilox (Bois, C. et al., 2012). During flexographic printing, the roller pressure is basically around 100 Pa; it is based on several parameters such as the nature of roller material that will affect the speed of printing, the material of substrate, the distance of impression and its hardness (Nash et al., 2015).

2.3.3 Doctor-blading

Doctor-blading method will be used to deposit the layers of ink on the substrate in this experiment. As stated by Krebs, F. C. in 2009, this technique can produce the films' formation with a well-predefined thickness; in the range of 10 μm to 500 μm as well as the loss in ink can be reduced to less than 5 *wt*%.

In this method, a sharp blade is placed at a specified distance above the substrate surface, also for both flat and groove surfaces. The ink is put in front of the blade and then the blade is moved linearly across the substrate. The value of the thickness of the coated layer is affected by the meniscus between the wet films on the blade trailing edge and the blade due to the blade speed (Nash et al., 2015).

According to Nash et al., other aspects that can affect the thickness of films are the surface energy of the substrate and/or its porosity, while the ink viscosity and its surface tension are also included. The final dry of the film thickness as being mentioned by Krebs, F. C. in 2009, will be proportional to the concentration of the solid metal presence in the solution and the width of gap while, the linear speed in this process can be ranged from 1 mm s^{-1} and 100 mm s^{-1}, which related to small shear stress during coating. Another representative for this method is by bar-coating that has the same way but their difference is that the ink is rolled by a bar over the substrate (Zheng, G. et al., 2013).

2.3.4 Gravure printing

In 2013, Hrehorova, E. et al. represented that gravure printing has four basic elements (Figure 2.2) to each unit of printing; impression roller, doctor blade, ink fountain and an image carrier (engraved cylinder) which the carrier itself is used to deliver the image that will be printed.

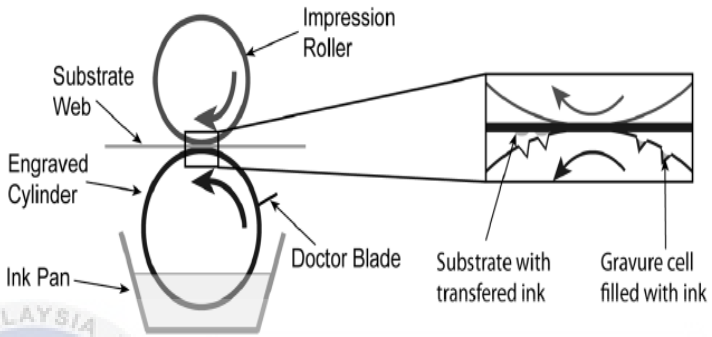

Figure 2.2 Basic positions of elements in gravure printing
(Hrehorova, E. et al., 2013)

Some of the benefits that make it an appealing procedure to print the electronic layers consist of its capability to print a wide thickness of ink track and to deposit low viscosity inks; thus it can be applied for a wide range of ink composition as well as substrates. In addition, it can produce a printing with great resolution and a long-term stability at increasing printing speeds. It also has the image carrier that comes with the solvent resistance and a special characteristic that other printing methods lack of.

2.3.5 Screen printing

In 2012, Kazani, I. et al. explained that screen printing was found at the end of the 9th century; where it is applied on almost all materials for instance wood, metal, paper, polypropylene, polyethylene, glass, ceramics and textiles.

With this cheap and simple procedure of printing method, a design is forced on a fine mesh screen, which carrying blank regions coated with a waterproof substance. Next, by shifting a squeegee passed the mesh, the ink is pressed through the mesh onto the square of printing (Kazani, I. et al., 2012).

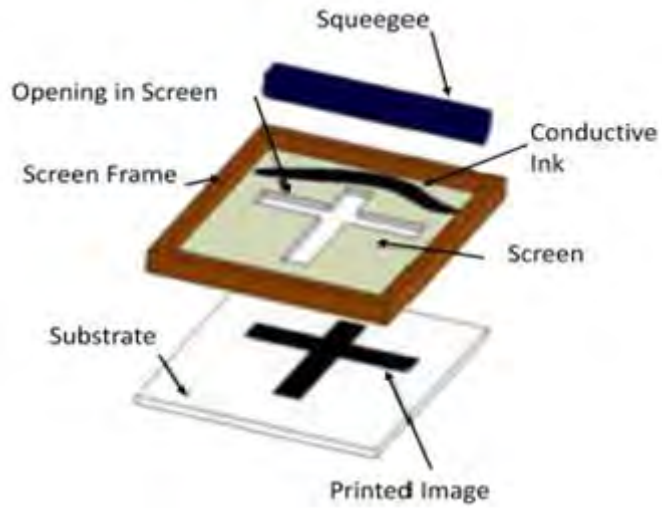

Figure 2.3 Basic principle of screen printing (Kazani, I., 2012)

2.3.6 Ink-jet printing

As stated by (Andersson, H. et al., 2013; Smith, P. J. et al., 2006), ink-jet printing process is a new method used and also known as the drop-on-demand (DOD) technique where it has the benefit of transferring controlled little amounts of ink onto the substrate producing the required pattern with less waste of ink. There are many commercial DOD-based inkjet printers utilizing thermal, piezoelectric, electrostatic or acoustic techniques of droplet generation (Kamyshny, A., et al., 2011)

The electrical resistance decreased abruptly with either the increasing of heating temperature or the number of overprinting which in terms of the resistivity and the number over printing, the most compatible number could be higher than 6 to gain high conductivity patterns at a low sintering/curing temperature (Shen et al., 2014; Cao et al., 2017).

One of the disadvantages of inkjet printing is that occasionally it is hard to obtain nice print quality with inks on the substrates caused by only the formulated ink with special characteristics can be used with ink jet print heads (Andersson et al., 2012). Other than that is the ink-jet is hard to control compared to the standard screen printing (Gierczak et al., 2016).

2.4 HEAT TREATMENT

As stated by (Jan Felba et al., 2013; Kamyshny, 2011), the inks are nonconductive just after the printing, and in order to gain a conductive ink with high conductivity, they need an additional post-printing treatment, mainly provided by a heating process. Heating or thermal procedure affects the resistance, and after the procedure, the resistivity of printed structure can be just a little higher that the bulk value of the material (Jan Felba et al., 2009).

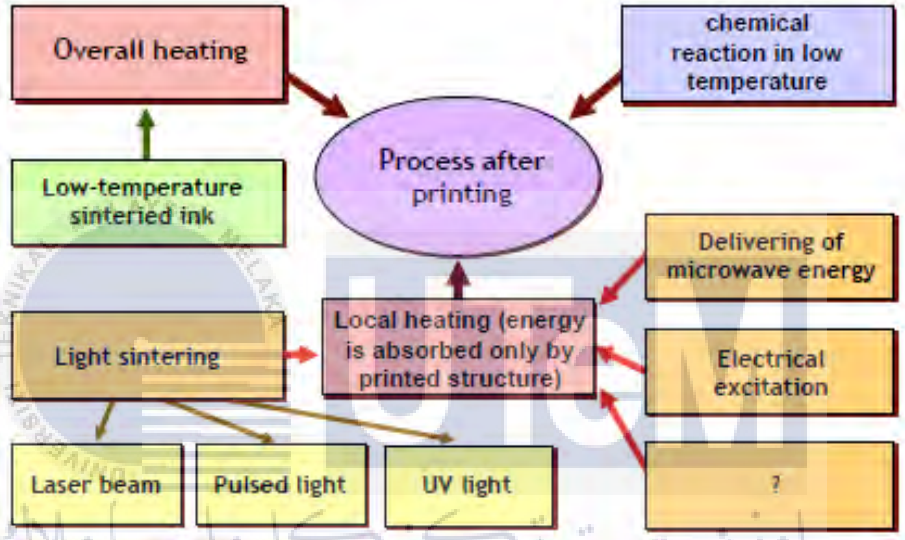

Figure 2.4 Options of processes after printing (Jan Felba et al., 2013)

In the aim of achieving high electrical conductivity, it is important for the silver nanoparticles to be cured or sintered, which can be done by electrical sintering, by thermal heating in oven or by any other techniques in order to remove the organic between silver nanoparticles (Allen, M. L. et al., 2008; Wang, Z. et al., 2017). According to Ismail, M. and Jabra, R., the critical curing temperature and the time of sintering influence the resistivity of printed patterns.

2.4.1 Sintering

According to Nir, M. M., Zamir, et al., sintering is a procedure of binding particles together at temperatures below their melting point. The sintering was more well defined at a higher temperature, proved by producing the lower resistivity (1.1 – 3 times of that bulk metal) when the printed patterns are sintered at temperatures above 200 – 250 °C, up to 400 °C (Chen, X. et al., 2010; Lee, K. J. et al., 2006). As stated by Ahn, B. Y. et al. in 2009, it has been recorded that silver nanoparticles can show high conductivity when being sintered at range of temperatures 200 °C – 350 °C.

The sintering procedure can be done by the exposure of the printed pattern to plasma, microwave radiation, intense light (photonic sintering), heat (thermal sintering), by chemical agent at room temperature (RT sintering) and by an electrical voltage application.

2.4.1.1 Plasma sintering

It is done when the printed patterns being exposed to electron-cyclotron resonance (ECR) plasma and low pressure Ar plasma (Reinhold et al., 2009; Ko et al., 2005)

2.4.1.2 Microwave sintering

This method as being said by Kamyshny is accomplished when the object dimension is perpendicular to the incidence plane is in the similar order as the depth of penetration.

2.4.1.3 Photonic sintering

According to Kamyshny, the process involved with the printed metallic layers absorbed the light and then the liquid evaporated, thus sintered. Local laser heating as shown in figure below, can be a benefit due to it is applicable for plastic electronics application, more productive energy transfer and reduced the heat-affected zone (Ko, S. H. et al., 2007).

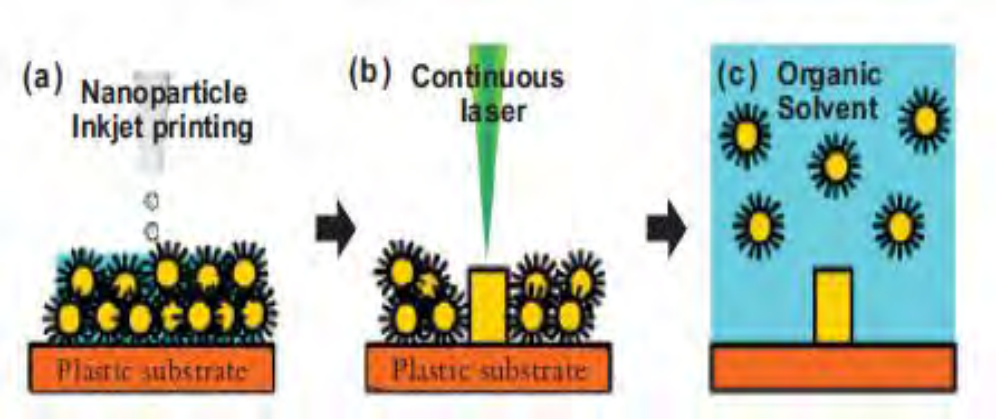

Figure 2.5 Inkjet printed by scanning through a focused cv laser on a polymer substrate (Ko, S. H. et al., 2007)

In 2007, Ko, S. H. et al. described that from the Figure 2.5, the column resembles a conducting site of a pattern being sintered while for circles, they resemble Au nanoparticles within a self-assembled monolayer and or unsintered nanoparticles, a proper solvent can wash them out.

2.4.1.4 Thermal sintering

According to Kamyshny, heating of printed patterns leads to the evaporation of liquid and the particles tends to be close each other. Basically, to distinguish all organic contaminants; heating at high temperature up to 300 °C and above is needed and the conductive patterns are hardly achieved at low temperature down to as low as 150 °C (Gamerith, S. et al., 2007).

2.4.1.5 Room temperature sintering

As stated by Kamyshny, metal nanoparticles faced a spontaneous coalescence procedure when they are in contact with oppositely charged polyelectrolytes which lead to producing high conductivities even at room temperature.

2.4.1.6 Electrical sintering

Allen et al., described that the procedure started when a voltage is applied over the printed structure which leads to flow of current through the structure, causes a local heating by energy dissipation. Kamyshny added that the benefits of this technique are decreased heating of substrate and small sintering time (in the range of microseconds to tens of seconds) as well as it is applicable to MC inks, if joined with thermal treatment.

In the figure below from Allen, M. L. et al., the detailed SEM images indicate that the samples from oven-sintered (Figure 2.6(b)) present tiny transformations of structural from the unsintered samples (Figure 2.6(a)), while the electrically sintered (Figure 2.6(c)) displays remarkable growth of neck and the size of grain.

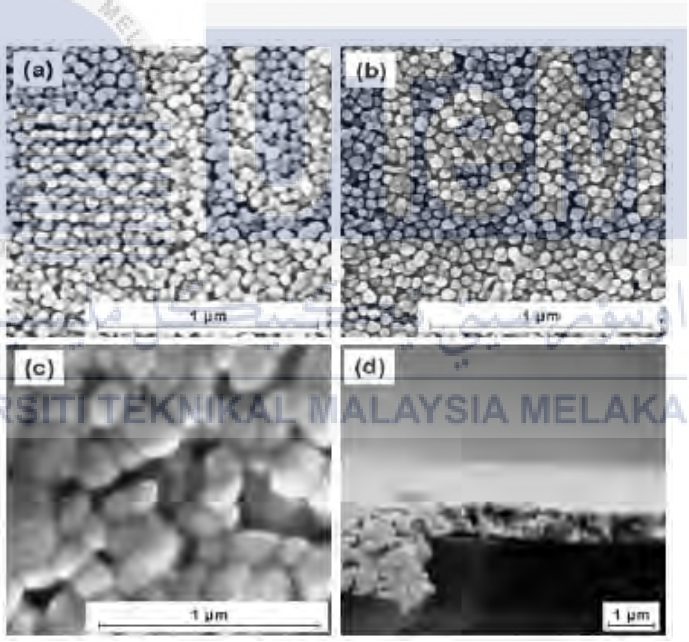

Figure 2.6 SEM images of printed nanoparticles (Allen, M. L. et al., 2008); (a) unsintered, (b) thermally oven-sintered, (c) electrically sintered and (d) cross-sectional view of the samples from (c)

2.4.2 Curing

As stated by Merilampi, S. et al. in 2009, after the patterns are printed, it is necessary to cure their layer as to produce high conductivity silver ink and to remove excess solvent. The printed silver patterns were sintered in the argon oven (Ismail, M. and Jabra, R., 2017).

Merilampi, S. et al. mentioned that a curing process can produce high adhesion of silver ink tracks on the substrate. Ismail, M. and Jabra, R. added that the silver nanoparticles start to melt and connect with each other to produce conductive paths; for instance, the silver ink is printed on glass substrate as shown in figure below, where the droplets merge into a steady substrate pattern which marks that as-prepared silver inks show a great adhesion on the glass, also a good printability.

Figure 2.7 Printed track of silver nanoparticles ink on glass slide (Ismail, M. and Jabra, R., 2017)

2.5 MATERIAL OF SUBSTRATES

According to the Dang, M. C. et al., adhesion between the ink and the material of substrate is one of the basic factors in producing conductive structures in printable electronics and the ink should be going through heat treatment at temperatures below 150 °C, or better 120 °C in order to be suitable with flexible substrates.

There are two options to develop the adhesion between organic substrate and silver ink; which are surface treatments of substrates such as UV-ozone, plasma or corona to increase the surface energy which leads to the improvement of an ink wetting, and the second option is to control the silver ink composition. For high adhesion implementation, it is important to have a low contact angle as close as possible to 0° and a great wetting (Dang, M. C. et al., 2014).

2.5.1 Glass substrates

For printed electronics, substrates that come with greater dimensional stability than polymer or paper substrate has the ability to upgrade device operation, registration and resolution (Hrehorova, E. et al., 2011). Glass slide will be used as a base substrate to find the best formulation of ink in the experiment.

Hrehorova, E. et al. classified that glass has been applied in the electronic field for being a very appealing substrate for very sensitive materials commonly used in organic printed electronics in which caused by its features; a) great resistance to moisture and oxygen, b) chemical barrier, c) good quality of surface and d) highly stability of combination between thermo-mechanical.

2.5.2 Paper substrates

In 2014, Öhlund, T. explained that paper-based substrates for printed electronics are captivating for its being cheap, flexible and environmental friendly, but it is also inconsistent and fibrous which is the major problem of applying paper as a substrate.

Other than that, surface roughness of uncoated paper and high porosity will cause the problem when the planned functionality is achieved. Paper is easily influenced by factors of environmental such as humidity and temperature that might affect the roughness and dimensional as well as the mechanical properties.

2.5.3 Polymer (flexible) substrates

Polymer substrates are widely used for printed electronics; unlike paper films, uncoated polymer substrates have no porosity, homogenous properties and smooth finishing. Although it brings various advantages in some topics, non-absorbing and smooth surface is non-satisfying in other topics (Öhlund, T., 2014).

In the description by Van Osch, T. H. et al., polytetraflourethylene (PTFE, Teflon) has great stability of temperature and resistance to chemicals and aging. But, somehow it is costly and has little surface energy that can generate challenges with "line bulging", which can be categorized as unneeded, a printed structure local widening.

Öhlund, T. mentioned that polyethylene terephtalate (PET), Polycarbonate (PC) and Polyethylene (PE) are mostly used as less expensive flexible substrates for printed purpose. Their points of softening are below 150 °C, thus they are not suitable with oven technique if high temperatures of sintering are required.

Chan, C. M. et al. presented that polyimide (PI, Kapton) substrates can maintain their flexibility and can resist the lengthen exposure to 300 °C. The high surface energy leads to a big wetting of ink, thus the smallest feasible structures can not be attained without decreasing the surface energy. The cost for this type of substrates is slightly expensive.

2.5.4 Polymer film and paper film

Table below shows the difference between polymer film and paper film in accordance to some properties or parameter.

Table 2.2 Comparison between Polymer Film and Paper Film

Property	Polymer Film	Paper Film
Smoothness of surface	Very high	Low
Mechanical Strength	High	Low
Chemical Stability	High	Low
Biodegradable	No	Yes
Absorbency	Low	Very high
Modification of Surface	Possible	Possible
Shrinkage	High	Low
Stiffness	Low	High

2.5.5 Stretchable substrates

In December 2006, Loher, T. et al. revealed that stretchability is found in the electronic field by the application of appropriate materials of stretchable substrate such as electronic elements and carriers. Among the discovered materials of stretchable substrate suitable for the assembly of electronic purposes, thermoplastic polyurethane (TPU) is one of materials that has the most potential (Loher, T. et al., 2006).

Loher, T. et al. also added that TPU can be chemically altered to satisfy the required physical characteristics as well as the combinations related which the versatility and the structure of base of TPU produces barrier to the bad weather, tearing, abrasion, impact and hydrocarbons as well as generates suitable compression and great resilience plus it can reach elasticity and a wide range of hardness although the add-on plasticiers are absent.

Loher, T. et al. figured out that the connection of electronic parts on the stretchable printed circuits depends on the procedures which can be found in traditional fabricating of printed circuit; etching, photostructuring and laminating for instance, the lamination of thin sheet of copper (Cu) onto the stretchable substrate as in Figure 2.8.

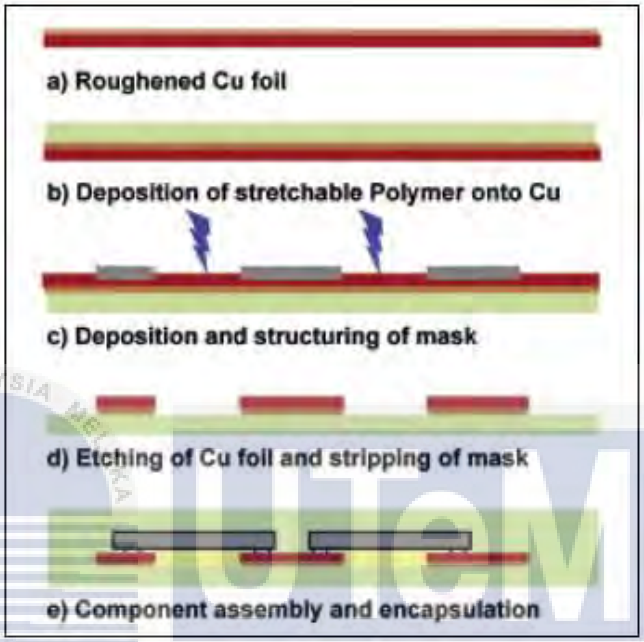

Figure 2.8 Procedure for the lamination of Cu on stretchable substrate by technique of printed wiring board (Loher, T. et al., 2006)

For stretchable substrates (Loher, T. et al., 2006), they are able to resist the temperature up to 180 °C only for a small amount of time and the precision of positioning on them are potentially to quibble and disfigure in consideration of the elasticity.

2.6 CONDUCTIVE INK CHARACTERIZATION

Merilampi, Laine-Ma, & Ruuskanen explained that the purpose of the characterization of conductive silver ink is to find out the parameters that can be improved in order to accomplish the desired properties of the ink in accordance to the conditions decided by different applications.

2.6.1 Electrical properties

In 2011, Joshi, S. S. explained that the material resistance which against the electric current flow; influenced by the dimensions of materials (the shape, length and area of cross sectional) and chemically material composition. Joshi, S. S. added that the resistivity with SI units of Ohm-meter is corresponding to the conductivity with SI units of Siemens/meter.

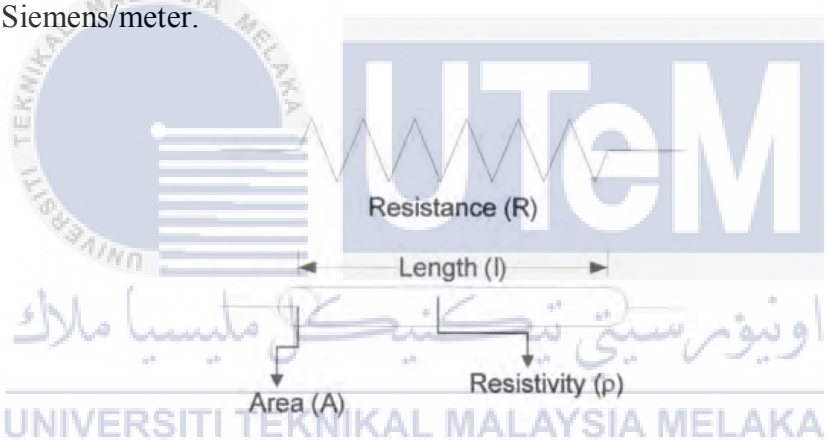

Figure 2.9 Material resistance (Joshi S. S., 2011)

The resistivity of the samples traces were obtained using the formula:

$$\rho = RA / L \tag{2.1}$$

Where ρ is the resistivity, A is the cross-sectional area of the ink, L is sample trace length from end to end and R is the resistance recorded from the multimeter (Jiang, S., 2017).

The measured values of resistance after each sample being dried were used for the next calculation for resistivity of the sheet by the equation:

$$R_{SH} = R \cdot W/l \tag{2.2}$$

Where l is the length of line in mm, W is the width in mm, R is the resistance in Ohm (Ω) and R_{SH} is the resistivity of the sheet in *Ohm/sq, Ω/sq*.

According to Nash et al., the resistance of patterns was determined by using a 4-point probe; when the probes were positioned on each of the lines, the current between the outer pins was set to I = 100 mA, and the voltage V across the inner pins being recorded. The resistance per unit length *(l)* was obtained by:

$$\frac{R}{l} = \frac{V}{I} \tag{2.3}$$

where the resistance per unit length is multiplied by the cross-sectional A in order to obtain the resistivity, ρ (Nash et al., 2015).

2.6.2 Conductivity versus temperature

In 2008, with the formation of an on-going percolation network throughout the printed pattern and the presence of metallic connection between the particles, the conductivity will increase as claimed by Perelaer, J. et al. Nevertheless, Maissel, L. I. and Glang, R. added that the presence of a thin (as of a few nanometres) residual organic layer among the particles of silver is adequate to avoid the movement of electrons between the particles. A rise in the temperature should distinguish the adsorbed dispersant that is possible to remain on the particles' surface (Perelaer, J. et al., 2008).

To acquire the possibly lowest resistance of the printed patterns, Perelaer, J. et al. proposed that the process of sintering is needed to convert the initial tiny contact regions to thicker necks, and finally to a dense layer; proved by Kim, D. and Moon, J., 2005 that the higher temperature causes the neck size grow by additional densification thus while this process is carried out, the connections among the particles become wider which leads to the increasing of conductivity.

2.7 SUMMARY

From the study of literature review, the knowledge about the type of materials, formulation of ink, methods of production to fabricate ink and the parameters investigated have been identified.

In order to proceed to the next chapter, the steps on how to conduct the experiment must be made using the information from this chapter. Silver nanoparticles will be used as the filler element to produce ink throughout this project and doctor-blading method will be applied to deposit the layer of ink on the substrate, also the glass slide will be used as the baseline. Furthermore, relationship between the materials and methods of study through parameters also can be found out once the literature review about the related topics has been studied.

CHAPTER 3

RESEACRH METHODOLOGY

3.1 INTRODUCTION

In this chapter, the method for the fabrication of the conductive ink, the materials and apparatus used and type of tests that was carried out on the conductive ink in this research experiment were described. Figure 3.1 is the summarized methodology in this study where it represents the flow of the research begins with the literature review study until the writing of final report in completing the project. The research flows related based on the overall flowchart that can be simplified into:

Section I : Data Collection
Section II : Sample Fabrication
Section III : Sample Characterization

In Section I, it started with designing the experiment procedures where the parameters were listed in formulating the sample (conductive ink) and followed by the processes of printing and curing. While, in Section II, it consists of the usage of 4-point probe, image analyzer (microscope) and contact profilometer in testing the behaviour of the sample produced.

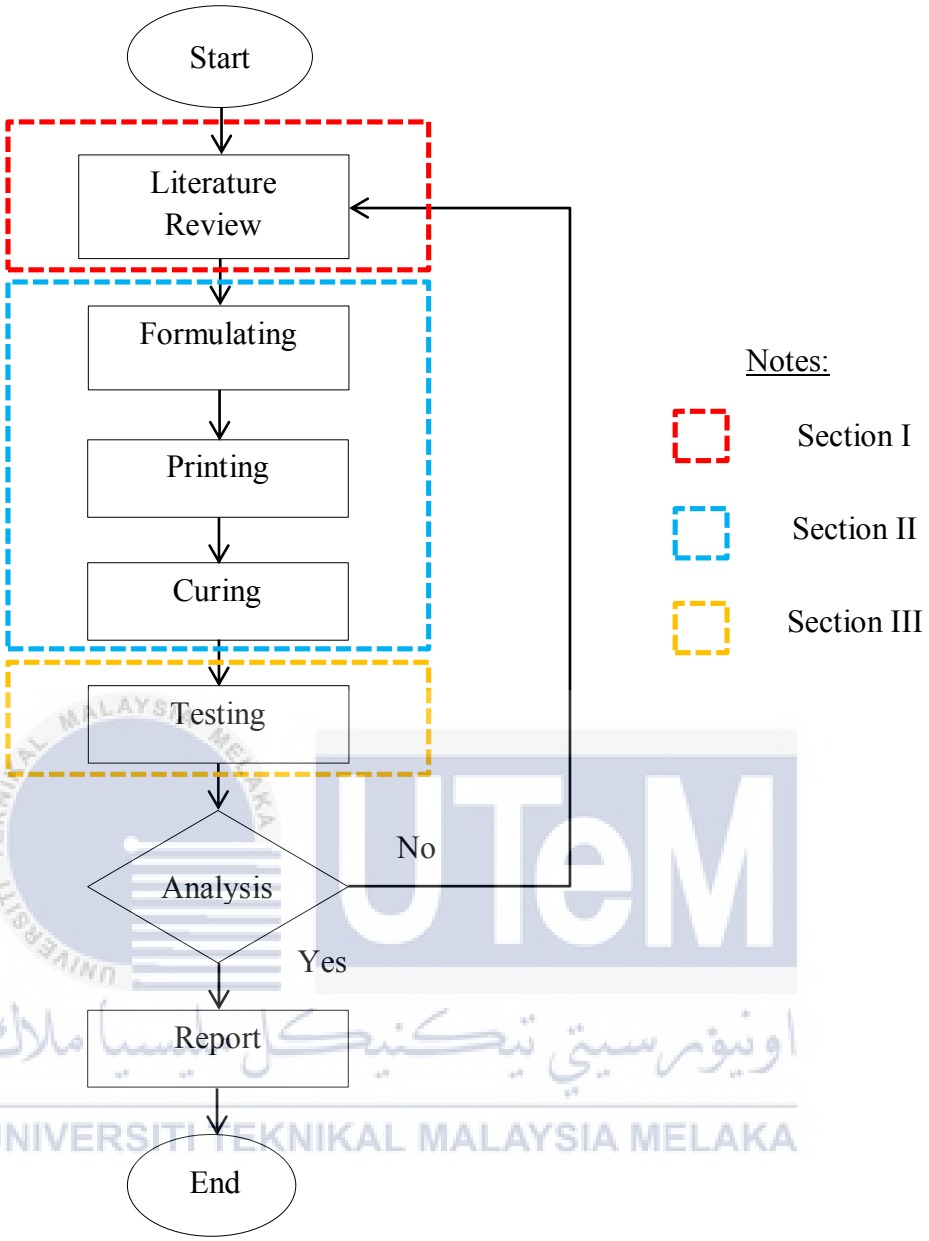

Figure 3.1 Methodology flowchart

3.2 DATA COLLECTION

The process of collecting data in this research is merely based on the study of literature review. The literature review is necessary as it gives the latest information about the subject being highlighted in terms of method applied, materials used, parameters being investigated and others from the previous research.

By referring to the literature review, the comparison between the past, present and the future study about the subject in this experiment can be identified thus; the potential weakness in this research potentially can be improved. From the comparison of the previous study, whole understanding of the subject should be obtained which will directly help to write the research report efficiently.

3.3 RAW MATERIALS

To produce the samples of conductive ink in this experiment, the materials involved were prepared as listed in the table below.

Table 3.1 Materials used

Materials		
Silver nanoparticles (AgNPs) 	Epoxy 	Hardener 
Used as the filler element	Used as the binder element, to bind the particles together	Used to harden or dry the mixture

3.4 SAMPLE FABRICATION

3.4.1 Formulation of ink

For the formulation of conductive ink in this experiment, the materials used were shown in the Table 3.1 and they were composed of various percentages in accordance to the Table 3.2.

Table 3.2 Composition of ink loading

Sample	Filler		Binder		Hardener (g)	Total (g)
	(%)	(g)	(%)	(g)		
1	10	0.2	90	1.8	0.54	2
2	20	0.4	80	1.6	0.48	2
3	30	0.6	70	1.4	0.42	2
4	40	0.8	60	1.2	0.36	2
5	50	1.0	50	1.0	0.30	2
6	60	1.2	40	0.8	0.24	2
7	70	1.4	30	0.6	0.18	2
8	80	1.6	20	0.4	0.12	2
9	90	1.8	10	0.2	0.60	2

The composition started from the least percentage until the highest percentage. The loading of hardener is 30% off from the amount of binder loading. The total value from the table is the sum of the amount of filler loading and binder loading as the total value was decided before the formulation process started which is 2 g. To begin, the weighing process should be started first and the material and apparatus involved were listed in Table 3.3.

Table 3.3 Material and apparatus involved

Material/Apparatus	Descriptions
Digital Analytical Balance	To weigh the material
Beaker	Used for mixing and stirring processes
Scoop	As a transfer medium of the material

The door of the analytical balance was opened and the beaker was put on the centre of the weighing pan (Figure 3.2) but not with bare fingers as the fingerprints will affect the required mass of the materials. Then, the door was shut and a few seconds were considered for the unit to stabilize. In order to obtain a precise readout of the substance being weighed, the weight of the beaker was cancelled out with the tare button was pressed until the display screen exhibited 0.0000 g.

Figure 3.2 Beaker positioned on the centre of pan

After the 0.0000 g was achieved, the door was opened and the materials being weighed were carefully added or reduced until the display exhibited the required weight in accordance to the value of weight in the table as shown in the figure below.

Figure 3.3 Value of weight being adjusted

But the weight should be slightly higher than the desired value; within tolerance of +0.05 g as the loss of weight of the materials was taken into consideration mixing them together. The described process was repeated three times as there are three materials involved for each sample.

3.4.2 Mixing and stirring processes

In this operation, there are some crucial steps before the final sample can be achieved and those steps are mixing and stirring processes. The materials and apparatus that will be used were listed in the table below.

Table 3.4 Material and apparatus involved

Material/Apparatus	Descriptions
Glass rod	To stir the mixture
Container	To store the extra mixture produced
Desiccator	To store the dry mixture
Multipurpose wipe	Used in cleaning process by wiping the apparatus
Acetone	As a medium to clean the apparatus

After all of the materials related had been weighed as shown in Figure 3.4, they will be mixed together into one beaker. Since all of the materials have different viscosity, materials with lower viscosity which are AgNPs and the hardener will be poured into a beaker containing material with the highest viscosity which is the epoxy. The purpose of this mixing method is to prevent the loss in weight of materials with high viscosity as they tend to stick to the beaker while being poured due to their properties.

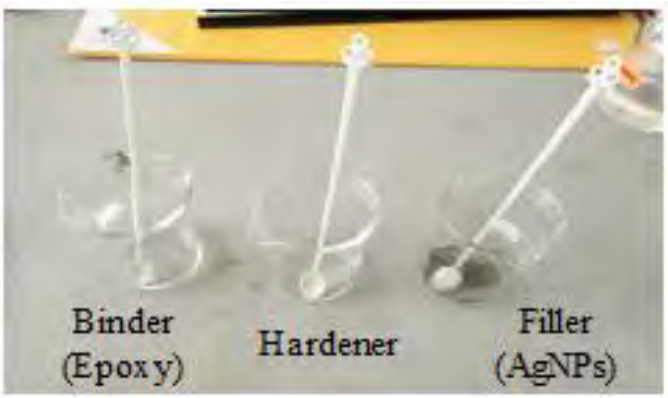

Figure 3.4 Materials after being weighed

The next steps to be taken was stirring process where in 2014, Shen, W. et al. continuously stirred the mixture of ink for one hour at 65 °C. For this experiment, the stirring process will take for five minutes continuously at room temperature by using a glass rod as can be seen in Figure 3.5.

Figure 3.5 Glass rod was used to stir

In order to obtain a well-dissolved mixture, the stirring process was proposed to be in one direction either clockwise or anticlockwise and the speed to stir the mixture must be consistent throughout the stirring process. There was a change in the stirring time where for the samples of 1, 2, 3, 4 and 5, they were prepared by stirring the mixture for 5 minutes while the rest of the samples; 6, 7, 8, 9 and 10 were produced by 10 minutes of stirring procedure.

The extended stirring time from 5 minutes to 10 minutes was decided after the samples of 1, 2, 3, 4 and 5 had been cured where there had been the trace of uneven consistency recognized within the ink deposited on the glass slide will be discussed further in the next chapter.

Once the stirring procedure was completed, all of the mixture was stored in a container (Figure 3.6) labelled with their own filler loading and then they were placed into an electronic desiccator. Desiccator is a sealed cabinet that is used to preserve the dryness of the material placed inside the desiccator by absorbing the moisture.

Figure 3.6 Well-dissolved mixture in the container

After the overall processes were completed, all of the apparatus used were cleaned with acetone by soaking the multipurpose wiper into the acetone. Washing the apparatus used in this experiment is a bit stressful due to the mixtures' residue is hard to remove off since their consistency is a bit thicker. Next, the apparatus was wiped with the acetone-soaked wiper until it was fully clean and then being rinsed with the water and let to dry.

3.4.3 Printing process

Table 3.5 Material and apparatus involved

Material/Apparatus	Descriptions
Scotch tape	Used to create the ink gap on the substrate
Razor blade	Used to apply the ink on all over the gap
Glass slide	Act as the substrate

Before the printing process started, the gap of ink tracks in two positions, A and B was constructed on the glass slide by using the Scotch tape to create the space of 0.5 cm width on the glass slide as in Figure 3.7.

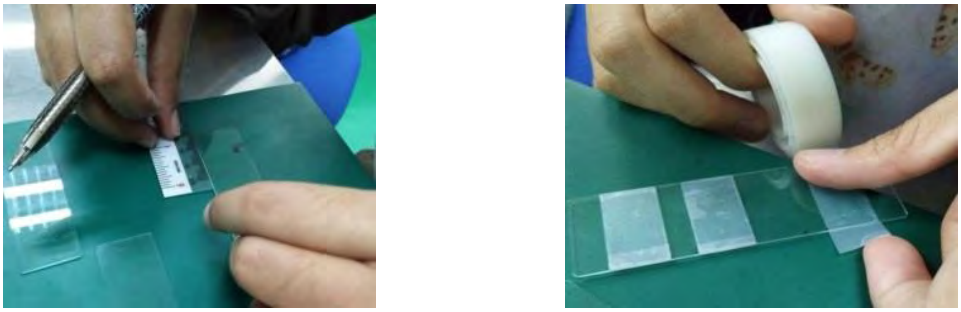

(a) (b)

Figure 3.7 (a) Constructing width of 0.5 cm (b) Applying the Scotch tape

Anand R. Maharaj wrote that the glass has high melting point as it is fully melted at the temperature range of 1400 °C up to 1600 °C based on the glass composition. Moreover, the glass does not conduct either heat or electricity. The substrate properties must be kept constant during the experiment so that it will not affect the outcome of this experiment.

Thus, the glass side is used as the substrate is for the purpose of ink characterization; to investigate the adhesion behaviour between the ink and substrate and to identify which composition of ink loading will produce the lowest resistivity in ink, thus indirectly the loading with best conductivity will be identified.

After the construction of tracks on the glass slide was completed (Figure 3.8), only then the printing process can be carried on. The method used to print the mixture of ink on the substrate in this experiment was doctor-blading technique; from this technique, the thickness and coverage of ink can be controlled manually.

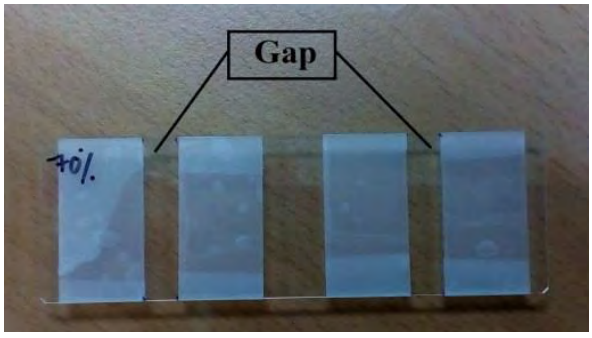

Figure 3.8 Constructed gap

In doctor-blading method, Nash, C. et al. described that the drops of ink were placed between two Scotch tape tracks to enable for a permanent gap between the substrate and the blade during printing as can be seen in Figure 3.9.

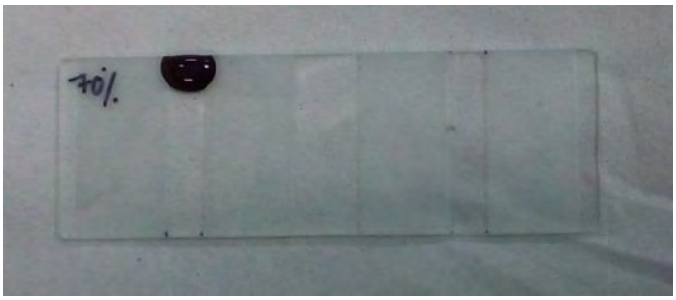

Figure 3.9 Dot of ink was put at the upper side

A sharp blade was used to move across the substrate at a constant speed of roughly 0.01 m/s (Nash, C. et al., 2015) so that there is fully ink coverage of the space. The blade was moved from the upper side of the gap towards the end of the gap in one move only as to ensure the distribution of the ink was the same on all over the gap and also the thickness of the ink as shown in Figure 3.10. The exact same steps can be repeated to adjust the coverage of ink over the gap until satisfied.

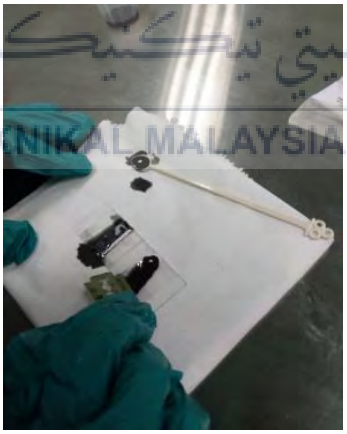

Figure 3.10 Blade was moved along the gap

3.4.4 Curing process

Curing process is needed in order to improve the bonding between the particles of filler, binder and hardener. Curing is also applied in purpose to melt the epoxy and to harden the mixture with the help of hardener thus, improving the adhesion between ink and the substrate.

Table 3.6 Material and apparatus involved

Material/Apparatus	Descriptions
Oven 	Heat source to cure the sample
Tray	Sample was put on it in the oven

In 2015, Matsuhisa, N. et al. revealed that curing temperature of more than 150 °C have exhibited the decreasing of the resistivity of metallic inks and resistivity of silver nanoparticles inks of 2 – 3 μΩ cm, only 25 – 88 % higher than bulk silver. Moreover, the melting point (T_m) of epoxy is above 177 °C thus, in this experiment; the oven was already setup with 160 °C and time of 1 hour during the printing process. The purpose of setting up the oven earlier instead of on the spot because the oven took some times to increase the temperature up to the desired temperature.

So, by setting the oven up earlier, the printed sample placed on a tray can be put into the oven just right after the printing process was completed, thus not affecting the sample in terms of external factors such as room temperature. After the printed sample was cured, it was then let to be fully dried at room temperature, thus the next procedure can be carried out.

(a)

(b)

Figure 3.11 (a) Inside the oven (b) Putting the tray into oven

3.5 SAMPLE CHARACTERIZATION

After the printed sample was fully dried, the sticky residue from the Scotch tape will be removed manually from the glass slide in order to view a well-defined track of ink before the analysis process was taken. Then, a number of marks were constructed on the glass slide next to the ink layer to indicate position of spot to be analyzed. Three marks were constructed at both ink layers in one sample indicating upper, middle and lower position to be characterized and the average values from these marks will be the final result in the data that will be discussed in details for the next chapter.

3.5.1 Microscopy

In 2013, Lu, K. defined the microscopy as a method that provides the measurements of particle shape and size, morphology and the dispositions of nanoparticles by producing two-dimensional pictures of three-dimensional items.

Figure 3.12 Microscope connected to computer

The microscope used in this experiment was connected to the computer so that the images from the microscope will be directly displayed on the screen. The sample was placed on the stage and it was held by the stage clips as can be seen in Figure 3.13 (a).

The revolving turret was turned in order to secure the position of the required power objective lens. In this experiment, three power objective lens were used which are 5x, 10x and 20x. Next, the focus knob was turned to move the stage upward or downward without having the objective lens in contact with the sample until the light was directed to the desired position (Figure 3.13 (b)), for instance, at position labelled 1. The focus knob was turned until the image has been into focus mode.

(a) (b)

Figure 3.13 (a) Sample was held by stage clips (b) Light was directed to the position

After a clear image of the sample was obtained, the image was recorded in the computer and the scale of the image was set up in 100 µm. Those described steps were repeated for another power objective lens as at each point; three images with different resolutions (5x, 10x and 20x) were required in this experiment.

Figure 3.14 Image was recorded

3.5.2 Electrical testing

Four point probe can be used to measure the sheet resistance value of the sample in ohms-per-square, the resistivity volume in ohms-cm and the thickness of sample. Four point probe works by forcing a constant current along two outer probes and next, the voltage is read out from the two inner probes.

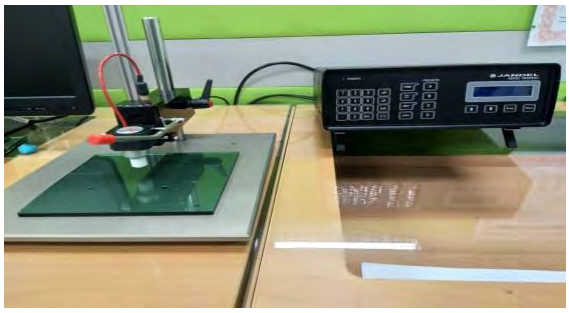

Figure 3.15 Four point probe with display meter

Before the resistivity measurement of the sample was taken, calibration for a reference sample should be the first to carry out. An indium-tin-oxide (ITO) coated glass was used as the reference sample to ensure whether the four point probe system is working well or not.

The reference glass was put on the base plate (Figure 3.16) and the pin of probe was lowered until 'tik' sound was heard which means it reached its limit. The height level was adjusted until it was in solid contact or touched the reference glass and waited for the measurement to be stable until the satisfied values of sheet resistance was achieved.

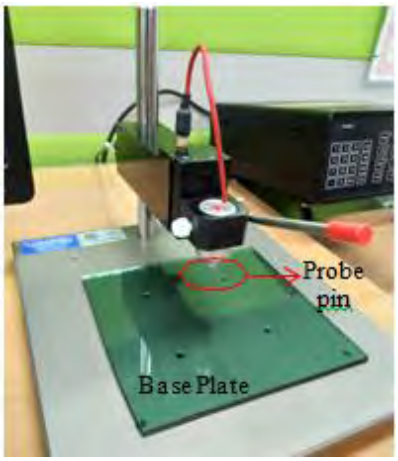

Figure 3.16 Base plate and probe pin

While doing the reference calibration, several measurements must be taken from random points across the central area of reference glass instead of from a fixed point. For the reference glass, their satisfied values from various random points must be a very stable and in agreement within the verified measurement of region, which is 12.55 ohms/square $\pm$ 0.25.

For the glass slide in this experiment, the same method as for the reference sample was used to obtain the values of sheet resistance. The sample was put on the base plate and the contact between the ink track and the probe pin was adjusted. Before the result of sheet resistance values was recorded, it must be in stable state and the suitable current has been achieved as it may take some times to reach the best current suited.

At each constructed points of the ink track, three readings of sheet resistance will be taken and the average values of them would be the result. Since each sample has two ink layers deposited and three points constructed at each layer, the total readings taken will be 18 of sheet resistance values for one sample.

However, the display meter will show comments such as “contact limit” or “out of range” may be due to poor contact; too close or no contact at all. Thus, an appropriate action should be taken in order for the display meter can read out the values. Poor contact can be detected through high standard deviations of several measurements taken from the similar areas which will be discussed for the next chapter.

3.5.3 Measurement of surface roughness

The surface roughness of the sample can be identified by using portable contact profilometer that was used to measure surface roughness of the sample. The measurement was taken at the same spot as microscopy and electrical used as shown in figure below.

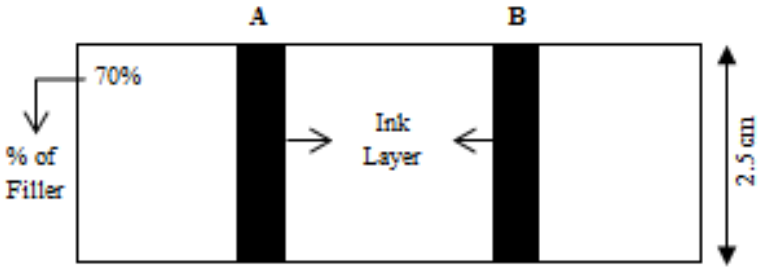

Figure 3.17 Sketch of sample

Each substrate has two samples of ink layers located side by side that was labelled as Position A and Position B. Furthermore, every position was divided into three regions; Region 1, Region 2 and Region 3. The measurement took place at each region, but in the case of measuring the surface roughness, the measurement was taken in two directions which were vertical direction and horizontal direction.

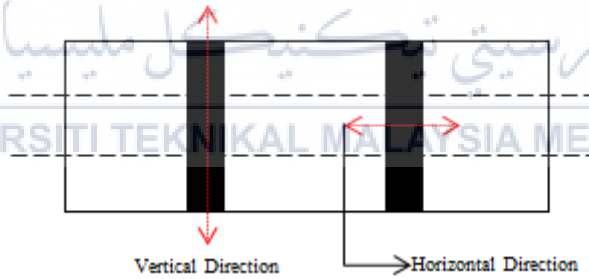

Figure 3.18 Region and direction of measurement

Figure 3.19 Measured sample

For the measurement principle, when taking the measurement of surface roughness, the sensor is put on the surface and then uniformly moved along the surface by driving the mechanism inside the instrument. Through the sharp built-in probe, the sensor captures the roughness of the surface. The roughness generates probe displacement which causes the change in inductive quantity of induction coils in order to produce analogue signal, which is in the part to the surface roughness at output end of phase-sensitive rectifier. The signal then enters the system of data collection and those collected data are processed with parameter calculation and digital filtering by the chip. After that, the results are being displayed on LCD screen.

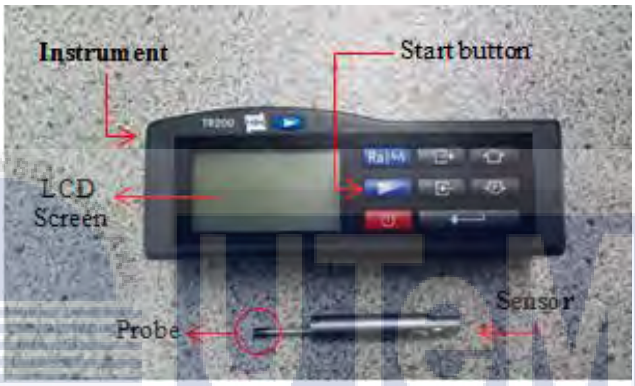

Figure 3.20 Instruments and sensor

Before measuring the surface roughness, suitable probe of the sensor must be chosen since there are two types of probe either for flat surface or curved surface. Then, the sensor must be installed into the connection sheath located at the bottom of the instrument as the first activity to carry out. The probe is the major part of the instrument and acquires careful handling where during the installation and unloading, the probe must not be touched so as to prevent disturbance of measurement data.

After the installation, the instrument was switched on and the related surface of the part was made sure to be clear. The instrument was placed (Figure 3.21) stable and correctly on the surface to be measured and its position including its height was adjusted so that the pin of the probe to be in contact with the surface. The sliding trail of the probe must be parallel to the direction of process line on the surface according to the required directions; vertical or horizontal.

Figure 3.21 Positioning instrument

Then, the Start key was pressed to start the measuring process and the pin was let to finish the sliding. While the pin was sliding, the instrument and the sample must be held firmly to avoid them from moving around; otherwise the movement may cause the reading to be “out of range” displayed on the screen. After sliding finished, the data was filtered and the instrument automatically stored the results; hence, displayed them on the screen.

3.6 SUMMARY

Since the formulation of ink has been decided before the experiment started, the experiment will be conducted based on 4Ms which are men, method, material and machine that has been stated in this chapter to fabricate the ink onto the substrate.

After the overall steps of ink fabrication have been made for all percentages of filler loading, the next step to be taken is the testing of the ink in terms of electrical properties and microscopy. Ink characteristic has been analysed by using microscope, four point probe and contact profilometer after the ink fully dried. Microscope was used to check the microstructure of the ink; the four point probe was used to check the resistivity of ink while the contact profilometer was applied to measure the surface roughness of the sample.

CHAPTER 4

RESULTS AND DISCUSSION

4.1 INTRODUCTION

In this chapter, the resistivity, the stability, the microstructure of ink and the surface roughness of the sample will be discussed to find out the best ink formulation based on the data gained through four point probe, contact profilometer and the images from the microscope.

4.2 ANALYSIS OF ELECTRICAL PROPERTIES

In 2014, Shen et al. concluded that the lowest resistivity of printed patterns of silver being sintered at room temperature was 8 μΩ cm that can be applied in many flexible electronics but, the resistivity can be reduced to 3.7 μΩ cm at increasing temperature of sintering up to 180 °C. After all, the resistivity can be reduced either by the number of printing cycles or by increasing heating temperature.

4.2.1 Result of resistivity

From the Table 4.1, A and B indicate the position of printed ink on the glass slide where it has two sides left and right where each side has three sample points where three readings of resistivity were taken at each point using four point probe.

Table 4.1 Resistivity results

% of Filler	Position	Resistivity (Ω/sq)								
		Point 1	Average	Total Average A & B	Point 2	Average	Total Average A & B	Point 3	Average	Total Average A & B
60	A	108.360	119.890	136.148	80.680	92.720	175.222	280.880	239.020	468.895
		118.720			122.190			312.740		
		132.590			75.290			123.440		
	B	148.330	152.407		301.420	257.723		528.570	698.770	
		141.820			281.530			774.820		
		167.070			190.220			792.920		
70	A	37.400	40.477	40.555	33.110	35.950	32.080	30.390	35.680	38.203
		42.460			34.320			40.770		
		41.570			40.420			35.880		
	B	43.050	40.633		33.090	28.210		43.370	40.727	
		39.960			28.140			45.280		
		38.890			23.400			33.530		
80	A	12.420	7.133	6.277	4.080	5.450	5.682	12.900	17.960	12.927
		5.410			4.180			19.300		
		3.570			8.090			21.680		
	B	7.030	6.277		5.280	5.913		9.590	7.893	
		6.420			6.820			4.950		
		5.380			5.640			9.140		
90	A	0.150	0.180	0.143	0.010	0.010	0.100	0.020	0.013	0.085
		0.170			0.010			0.010		
		0.220			0.010			0.010		
	B	0.030	0.107		0.160	0.190		0.140	0.157	
		0.130			0.280			0.140		
		0.160			0.130			0.190		

At 60% of filler, its average resistivity is the highest among four of the filler percentage; thus may produce lowest conductivity as the resistivity value is proportional to the conductivity value. The values at 70% was a lot lower than the values at 60%; as shown in the table, their values had big gap between each other despite their filler loading had no much difference in terms of percentage.

Moreover, graph in Figure 4.1 showed the total average resistivity against the percentage of filler loading. It displayed that even the formulation of ink used at positions A and B were the same; it still showed there was some differences in terms of their resistivity value. The graph indicated that when the percentage of filler loading got higher, the average resistivity will alternately to decrease as the amount of conducting materials in the sample increased.

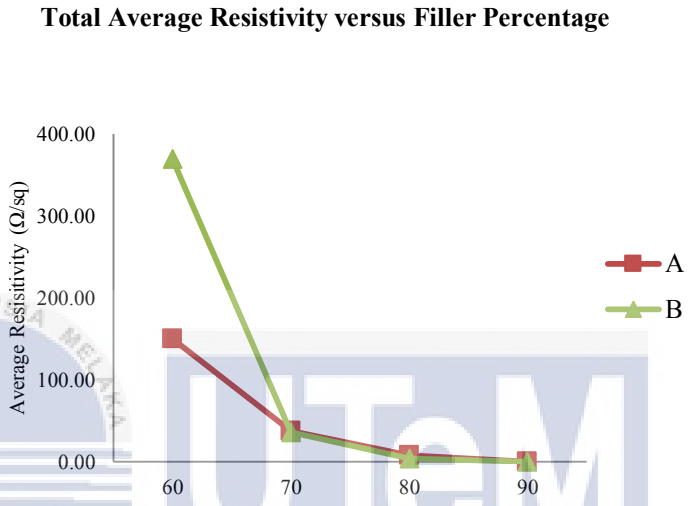

Figure 4.1 Graph of total average resistivity versus filler percentage

For filler at 80% and 90%, their average value of resistivity is gradually decreased with the increasing of filler percentage; being linked to the high amount of conducting materials composition in the ink. Being the filler with highest percentage of 90%, it may produce the highest conductivity among the overall filler percentages.

As for the filler composition of 10% up to 50%, four point probe did not detect any presence of resistivity value of the printed ink as it may lack of conducting materials' percentage in the ink. It proved that the lower the percentage of conductor filler, the lower the conductivity with increasing the resistivity as can be seen in Figure 4.1. Therefore, they were not included in data tabulating for this analysis.

4.2.2 Analysis of stability

In this analysis, there were two types of comparison, which were; comparison of standard deviation between filler percentage and comparison of estimation of error between filler percentage.

4.2.2.1 Comparison of standard deviation between filler percentage

There is no standard benchmark in determining the standard deviation, but to know the best standard deviation; it must be in the lowest value. It can present how tightly the data is gathered around the mean or average or how far the data is spread out from the mean or average.

Table 4.2 Standard deviation results

Filler (%)	Position	Standard Deviation			Overall Standard Deviation
		Point 1	Point 2	Point 3	
60	A	12.16	25.66	101.35	77.82
	B	13.11	59.30	147.68	289.86
70	A	2.70	3.92	5.19	2.69
	B	20.39	4.85	6.31	7.20
80	A	4.67	2.29	4.54	5.29
	B	0.83	0.81	2.56	1.04
90	A	0.04	0.00	0.01	0.08
	B	0.07	0.08	0.03	0.03

From Table 4.2, the data can tell that 60% of filler has a very large standard deviation which means the data is spread out widely from the average, indicated they have the highest average resistivity. The high range of values at 60 % is expected to be followed by 70% of filler but, it turned out that the values at 70% had major difference from the values at 60 % where it had one of the lowest values among the other filler loadings.

While for filler at 80% and 90%, the data has a small standard deviation telling that the data is gathered closely around the average, which proved that 80% and 90% of filler have the lowest and stable average resistivity.

4.2.2.2 Comparison of estimation of error between filler percentage

It is known that the data should obtain the standard *E* in the range of 5% and below. From Table 4, it presented that 60 % of filler had the highest *E* among all of the fillers, be it from Sample A or Sample B which means it was totally out of range from the standard *E*.

Table 4.3 Average estimation of error between filler percentage

Average Estimation of Error (%)						
Filler (%)	Position A			Position B		
	1	2	3	1	2	3
60	9.99	21.19	32.24	6.42	17.48	16.24
70	40.48	35.95	35.68	40.63	28.21	40.79
80	50.92	32.12	30.73	27.58	27.44	36.69
90	27.58	0.00	33.33	53.33	31.25	30.56

The estimation of error, *E* is calculated based on the equation:

$$E = \left| \frac{Resistivity\ at\ one\ point - Average\ resistivity}{Average\ Resistivity} \right| \times 100\%$$

For instance, to calculate the maximum estimation of error, *E* for Sample 1 at 60% filler loading from the Table 4.1:

Resistivity at point 1 = 108.36, 118.72, 132.59; Average resistivity = 119.89

Thus,
$$E = \left| \frac{108.36 - 119.89}{119.89} \right| \times 100\% = 9.62\%$$

$$E = \left| \frac{118.72 - 119.89}{119.89} \right| \times 100\% = 9.76\%$$

$$E = \left| \frac{132.59 - 119.89}{119.89} \right| \times 100\% = 10.59\%$$

Then, the average of $E = \frac{9.62 + 9.76 + 10.59}{3} = 9.99\%$

Filler at 70% is expected to have the least difference compared to the 60% of filler, but the data presented dramatic changes as the values had huge difference from the values at 60%, roughly 30% higher than values at 60%.

Then, for filler at 80% and 90%, they presented inconsistent value of *E*, there was some of 20 ~ 40 was in the range and some values were out of the range; 50.92% and 53.33%. The unstable range of *E* happened may be caused by two reasons; printing technique and four point probe measurement.

4.2.3 Sources of potential error

There are two sources of potential errors that had been presumed, which were due to printing technique and four point probe measurement.

4.2.3.1 Printing technique

In 2006, in order to produce fewer flaws of conductive tracks with good resolution, Kim, D. et al. proposed that there is a need to alter the silver ink composition and some printing states, consisting of the speed when printing which is linked to the firing frequency, the temperature of substrate and the inter-spacing interval among the dots.

In this case, the inconsistent range of *E* may be due to the printing technique; doctor-blading method. During the printing process, the ink may be not well-distributed all over the gap between the Scotch tape on the glass slide when the blade was moved across the gap due to the speed or the viscosity of ink.

When the speed of moving the blade is high, it may be the loss in ink where the ink may not cover all over the gap region. While for the viscosity of ink, as the filler content is higher, it will follow to increase as well. Ink with high viscosity was hard to be printed in compliance to the texture of ink; more concentrated texture.

Thus, it may affect the thickness of ink tracks printed on the glass slide. Some regions may have different thickness, thin or thick which leads to the different spreads of conducting material, silver nanoparticles on the substrate where region with high content of silver will have low resistivity and vice versa.

4.2.3.2 Four point probe measurement

Another factor of the instability in E is the time condition while taking the measurement using the four point probe. The error happened may be caused by there was no adequate time spent before taking the data. The time is needed due to RC (resistance-capacitance) delay in the highest resistive samples as the current requires some times to climb up to the value of saturation.

Once the data is stable, only then a certain point of measurement can be taken and the average value can be obtained. Hence, when the time spent is inconsistent, so does the resistivity value where it will be unstable too.

4.3 ANALYSIS OF MORPHOLOGICAL

Light microscopy was conducted on the sample ink tracks to investigate the ink track in a microscopic condition. In this section, all of the microstructure images were divided into three categories, which were microstructure with no conductivity, microstructure that should have conductivity and microstructure with conductivity. The microstructure images were organized in accordance to their filler loading with three scales of magnification; 5x, 10x and 20x.

Table 4.4 Microstructure with no conductivity

Filler (%)	Magnifications		
	5x	10x	20x
10	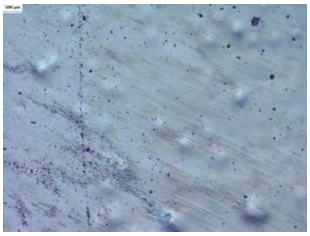	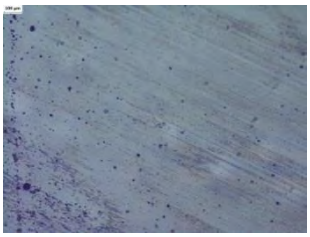	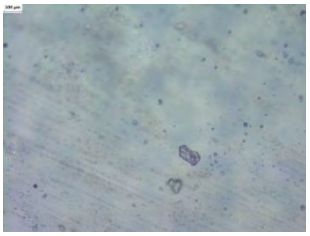
20	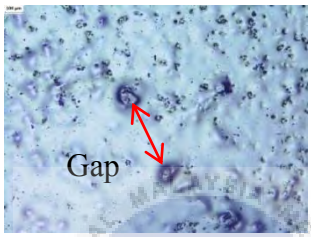	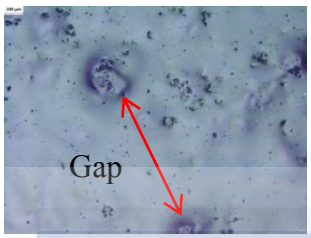	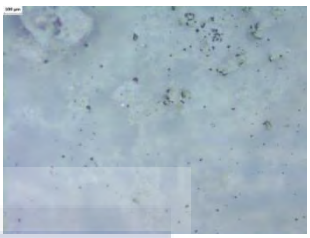
30	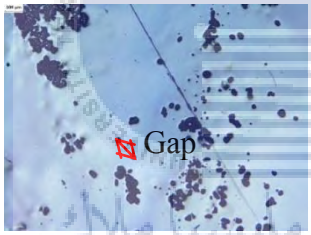	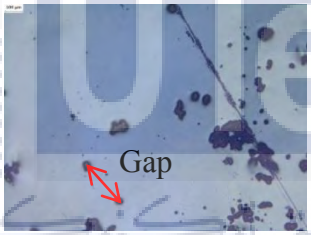	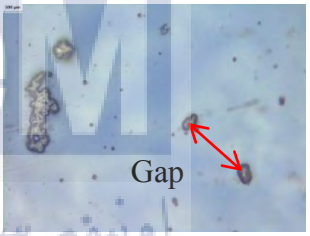
40		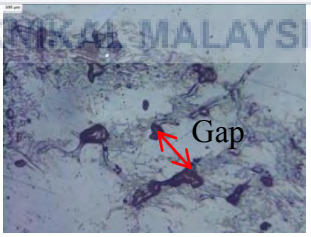	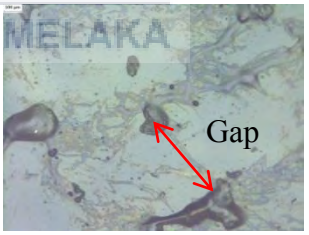
50	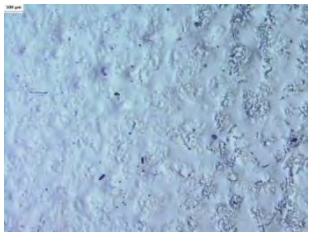	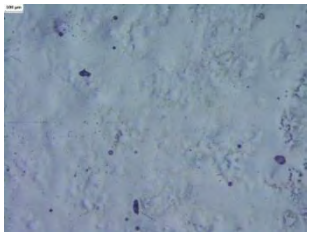	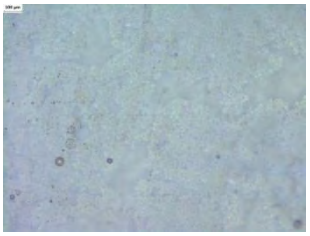

In Table 4.4, the microstructural transformation of the silver nanoparticles ink based on the filler loading in the range of 10% until 50% is shown. For 10% filler loading, the microstructure showed that there was no appearance of silver nanoparticles element has been traced due to lack of filler loading compared to the amount of binder and hardener as the binder and hardener have conquered all over the ink track and if the conductor materials are in low quantity (Nash, C. et al., 2015), there is no conductivity at all. Overall, the 10% filler loading only created the formation of voids as shown in Table 4.4.

While at 20%, 30% and 40%, there was the existence of the gaps between silver nanoparticles. It exhibited the frequency of gaps between silver nanoparticles that will affect the electrical properties of the conductive ink layer as the increasing gap number will cause the resistance to increase due to high voltage required to ensure there is current flow among the silver nanoparticles (Kazani, I., 2012). Next, percentage of filler loading of 50% showed the presence of silver nanoparticles but in a very small quantity may be due to the same ratio of filler to binder.

Table 4.5 Microstructure at 70% filler loading

Filler (%)	Magnifications		
	5x	10x	20x
70			

At first the 70% filler loading did not show any traces of conductivity although it was expected to have conductivity exists in the ink layer. Based on the microstructure images, there had been some traces of scratch developed in the ink layer which may be due to some mistakes happened during printing process as it was manually deposited onto the substrate. After multiple times of fabricating the ink with 70% filler loading, finally the trace of resistivity within the ink has been identified at forth times of try and error process.

Table 4.6 Microstructure with conductivity

Filler (%)	Magnifications		
	5x	10x	20x
60	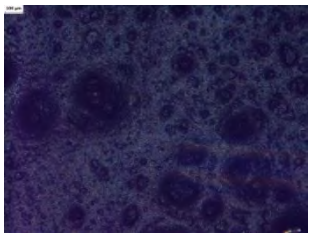	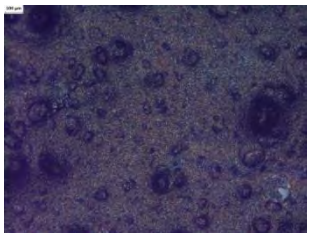	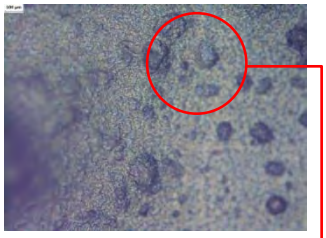 Granular particles
80		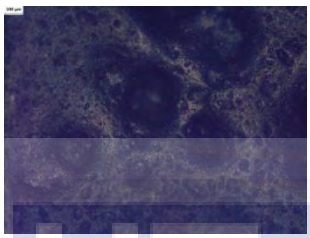	
90	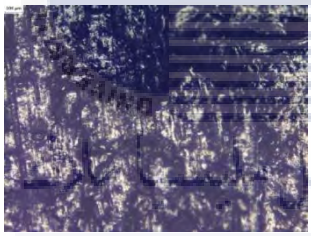		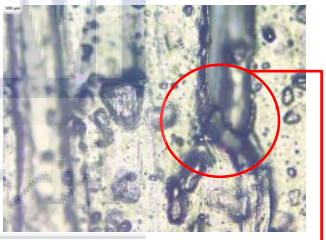 Continuous particles

From Table 4.6, it contained filler loading that has contributed the conductivity in the ink. For 60% and 80%, they displayed no outstanding difference between each other either in shape of particle or size compared to the filler loading at 90%. At 60% and 80%, the ink layer had the presence of granular-like particle and according to Kim, D., & Moon, J. in 2005, in order to be conductive ink, the granular particle should contain a 3D connection of conduction which leads to the existence of particle necking. Kim, D., & Moon, J. also believed that the necking growth provides a continuous connection and once the interparticle neck has been produced, the granular-like particle will be conductive although it is still porous.

At 90%, the dark colour in the microstructure represented the presence of silver while the brighter region was the binder once it has already been melted and major changes were noticed by Kamyshny, A. in 2011 as most barriers between particles have been vanished. This indicated that the ink layers have a close-packed structure where the particles created a strong bonding between each other. Once the silver nanoparticles were in contact between each other, the particles became more continuous rather than being in the shape of discrete and spherical, thus the contact area between particles became bigger.

Roberson, D. A. et al. explained that the increasing conductivity can be discussed only by bigger area of contact through the percolation theory. In 2017, Jiang, S. believed that the percolation theory reported that when electricity flows through the structure of silver nanoparticles, the electricity has a potential to percolate between each other and the probability is based on the sintering process, where the probability is very low until the best percentage is achieved and that percentage is known as the percolation threshold.

4.4 ANALYSIS OF SURFACE ROUGHNESS

In this study, Gökkaya, H. and Nalbant, M. explained that the parameter of surface applied to assess the surface roughness is the average of roughness, Ra that is also recognized as the centreline average (CLA) or arithmetic average (AA). The roughness average (Ra) is the integral of absolute value of the height of profile roughness over the length of evaluation, or the region between its centre line and profile of roughness (Gökkaya, H. and Nalbant, M., 2007).

4.4.1 Surface roughness in vertical direction

The results of the surface roughness for measurement in vertical and horizontal directions are shown in the table stated. All other parameters are remained constant so that only the surface roughness effect can be merely obtained.

Table 4.7 Vertical results

% of Filler	Position	Surface Roughness (μm)								
		Point 1	Average	Total Average A & B	Point 2	Average	Total Average A & B	Point 3	Average	Total Average A & B
10	A	0.249	0.235	0.281	0.259	0.273	0.276	0.108	0.099	0.114
		0.208			0.279			0.099		
		0.247			0.280			0.091		
	B	0.344	0.328		0.271	0.279		0.124	0.129	
		0.330			0.277			0.112		
		0.310			0.290			0.150		
20	A	0.784	0.834	0.689	0.295	0.290	0.229	0.124	0.141	0.111
		0.880			0.292			0.178		
		0.839			0.284			0.121		
	B	0.537	0.544		0.190	0.168		0.090	0.081	
		0.548			0.164			0.081		
		0.546			0.150			0.071		
30	A	0.922	0.909	0.686	0.933	0.910	1.033	1.803	1.746	1.097
		0.916			0.915			1.696		
		0.889			0.883			1.738		
	B	0.482	0.463		1.171	1.156		0.483	0.447	
		0.459			1.128			0.435		
		0.448			1.169			0.424		
40	A	0.696	0.768	0.561	0.398	0.426	0.364	0.306	0.317	0.300
		0.807			0.411			0.323		
		0.801			0.469			0.321		
	B	0.320	0.354		0.311	0.302		0.293	0.282	
		0.370			0.291			0.257		
		0.371			0.303			0.297		
50	A	0.285	0.286	0.245	0.247	0.241	0.240	0.367	0.383	0.383
		0.285			0.240			0.385		
		0.288			0.237			0.396		
	B	0.205	0.204		0.239	0.239		0.367	0.383	
		0.203			0.240			0.385		
		0.203			0.237			0.396		
60	A	3.409	3.509	4.264	2.709	2.726	4.006	2.300	2.349	2.319
		3.547			2.724			2.407		
		3.570			2.745			2.341		
	B	5.048	5.020		5.270	5.286		2.323	2.288	
		5.023			5.283			2.276		
		4.989			5.306			2.266		
70	A	3.977	3.753	4.434	5.014	4.981	3.736	2.890	2.850	3.257
		3.669			4.992			2.852		
		3.613			4.938			2.807		
	B	5.045	5.114		2.463	2.490		3.707	3.665	
		5.226			2.502			3.657		
		5.071			2.506			3.631		
80	A	5.266	5.378	4.299	3.509	3.397	3.461	2.271	2.254	2.169
		5.370			3.387			2.260		
		5.499			3.294			2.232		
	B	3.146	3.220		3.628	3.526		2.020	2.084	
		3.166			3.541			2.088		
		3.349			3.409			2.145		
90	A	5.220	5.199	5.721	5.192	5.477	5.890	4.700	4.490	5.716
		5.151			5.644			4.352		
		5.226			5.596			4.417		
	B	6.240	6.242		6.248	6.303		6.890	6.943	
		6.170			6.276			6.921		
		6.316			6.384			7.017		

Each of the data is translated into the graph that represents three types of relation; relationship between surface roughness and number of measurement taken on the same spot, relationship between Ra and point of measurement and relationship between total Ra and measurement points at both positions.

Table 4.8 Analysis of vertical results for 10% of filler

Vertical Results	Analysis
Position A	
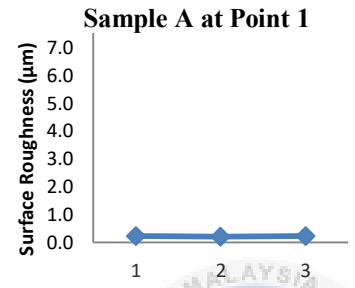	It has low surface roughness that is in range of 0.2 – 0.25 µm, which means that the result has stable consistency.
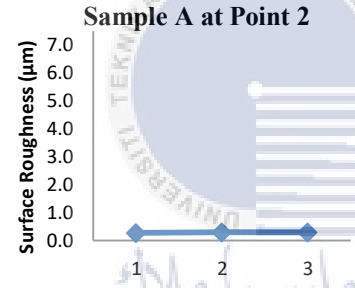	The graph illustrates low surface roughness where the range is 0.25 – 0.3 µm, but it increases compared to the previous point.
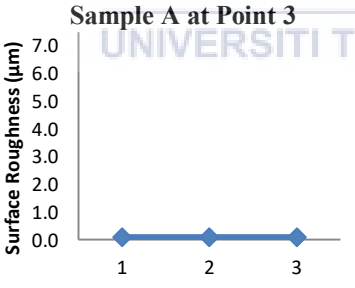	This area has the lowest surface roughness that is in range of 0 – 1 µm, which means that it has the smoothest surface.
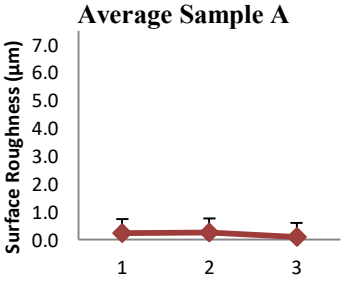	At point 3, Ra between three points is the lowest compared to the other two points, but the sample still has smooth surface. The error bar appears to be short since the difference between the highest and the lowest values at each point are 0.041 µm, 0.021 µm and 0.018 µm.

Position B	
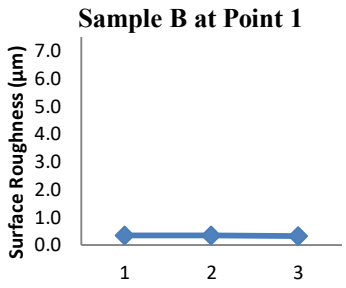	It has the highest surface roughness value compared to other points in both position, but in consistent range.
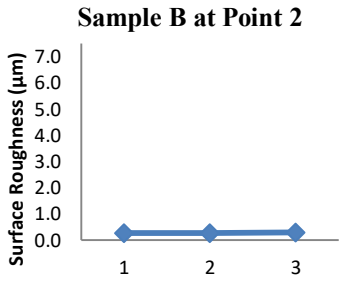	The graph illustrates low surface roughness with small gap of value between the times of data reading.
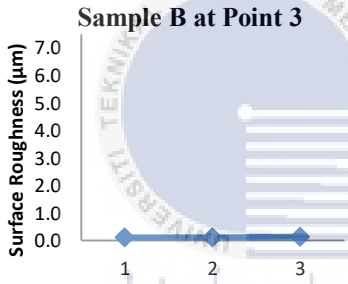	It has the lowest surface roughness value compared to the value in this position. At third reading when the data is taken, the value slightly increases.
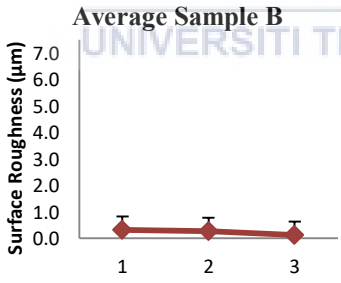	At the first and second points the data is taken, Ra is consistent while at the third point, the value decreases, but the sample is still in homogenous solution since the value gap is small. The error bar appears to be short since the difference between the highest and the lowest values at each point are 0.034 µm, 0.019 µm and 0.038 µm.
Total Average at Positions A & B	
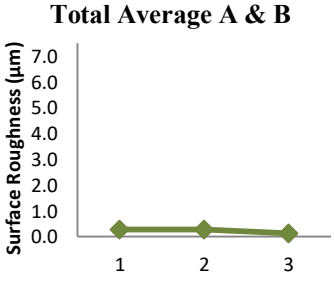	At point 1 and 2, total Ra is consistent while at point 3, it decreases in value but in small gap, which describes that the sample is in homogenous solution. The error bar is barely to see which proves that the total average values are more certain.

Table 4.9 Analysis of vertical results for 20% of filler

Vertical Results	Analysis
Position A	
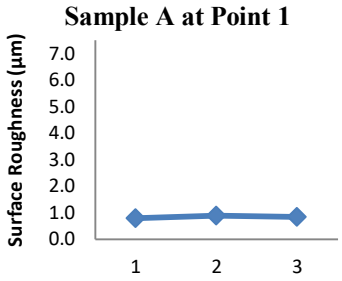	It has the highest value of surface roughness for 20% of filler, which is in the range of 0.7 – 0.9 µm.
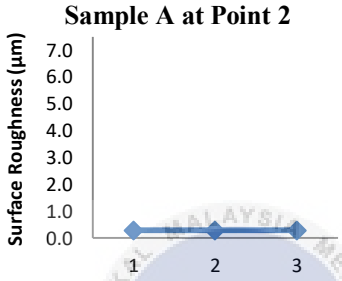	The value of surface roughness is consistent since the gap of value between the reading times of data taken is small.
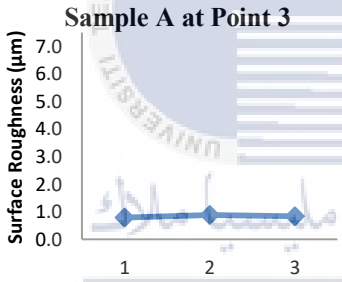	The graph illustrates the lowest surface roughness value at this position with the range of 0.12 µm until 0.18.
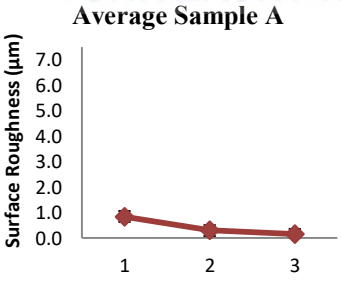	There is decreasing of Ra from the first reading to the second and third readings, obviously which the difference in Ra value between the first and second reading is 0.46 µm. The error bar is in small dimension which coming from the difference between the highest and the lowest values at each point are 0.055 µm, 0.011 µm and 0.057 µm.
Position B	
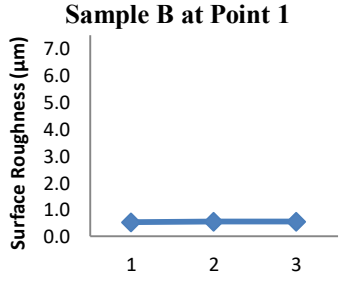	Graph illustrates that the value of surface roughness is the highest at this position where the data is 0.5 µm and above.

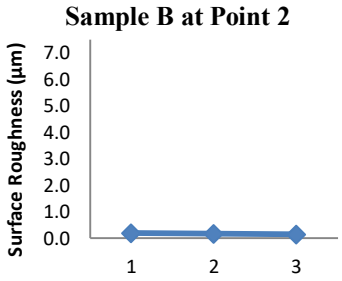	From the graph, the data from third reading shows slight decreasing of surface roughness value.
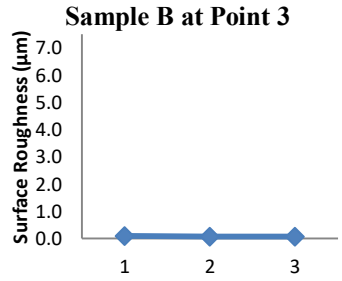	Graph illustrates that it has the lowest value range of surface roughness which is below 0.1 µm where the graph shows the consistency between the data.
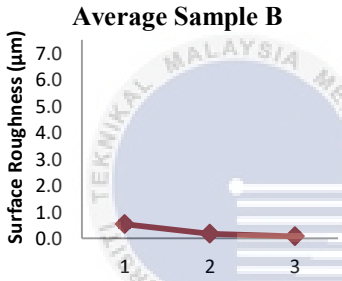	The same as at position A, Ra starts decreasing at point 1 from 0.689 µm to 0.229 µm; but between point 2 and point 3, there is small difference in their data. The error bar is barely to see since the difference between the highest and the lowest values at each point are below 0.04 µm.
Total Average at Positions A & B	
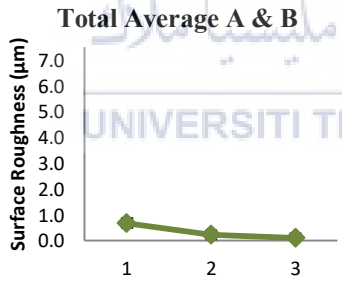	The graph displays similar condition with Average Sample A and Average Sample B where at the first point; total Ra starts decreasing but consistent at point 2 and point 3. The error bar is barely to see which proves that the total Ra values are more certain.

Table 4.10 Analysis of vertical results for 30% of filler

Vertical Results	Analysis
Position A	
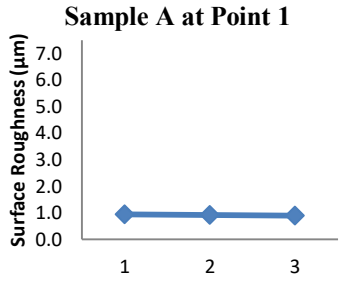	From the graph, the data can be seen roughly has consistency since the difference of surface roughness value between reading time is small.
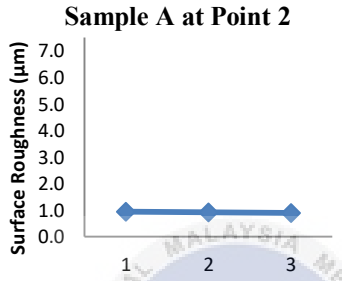	The graph also shows consistency since the gap between the surface roughness values is small but there is slightly decreasing value at third reading.
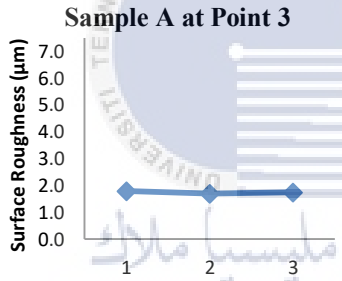	The data displays slight difference among all of the three readings since the range between the highest value and the smallest value is small.
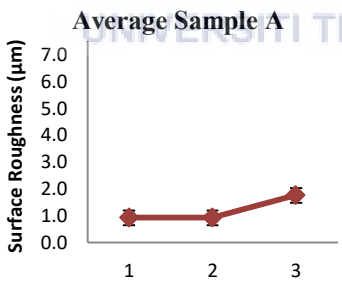	Through the graph, Ra starts to increase from Reading 2 to Reading 3 with the difference value of 0.836 µm while the data keeps consistent between the first and second readings. The error bar is in small dimension which coming from the difference between the highest and the lowest values at each point that is 0.107 µm and below.
Position B	
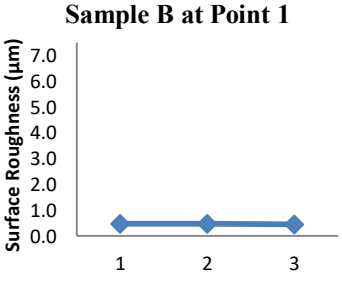	The graph is consistent since there is no big difference between their values of surface roughness.

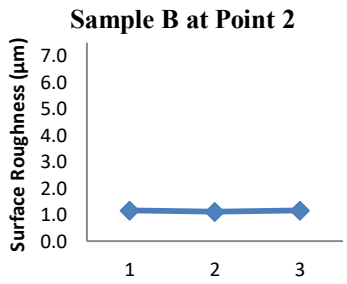	At first and third readings, the data is consistent, but for second reading, the data is a bit decreasing in value.
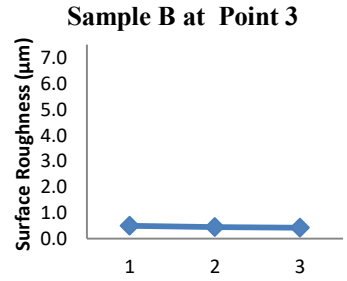	The graph also has same condition as at point 1 where the difference between the values of surface roughness is small.
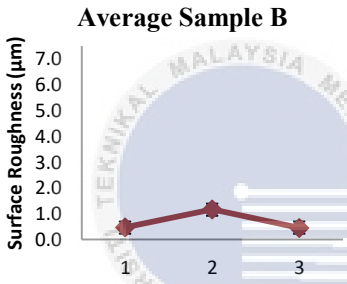	As can be seen in the graph shown, the Ra value from second reading has obvious difference compared to the average value from first and second readings. The difference value between Reading 1 and Reading 2 is 0.693 µm while between Reading 2 and Reading 3, the difference value is 0.709 µm thus there is no consistency in their values. The error bar is in short dimension which caused by the highest value is 1.171 µm and the lowest value is 0.424 µm.
Total Average at Positions A & B	
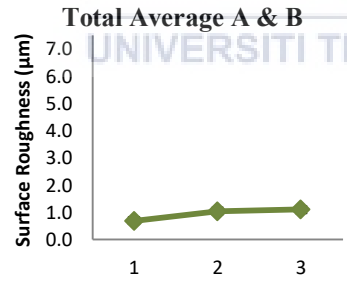	The total of Ra keeps increasing across the three points, but at point 2 and point 3; they have small gap in data. The error bar is barely to see which proves that there is small difference between the average values.

Table 4.11 Analysis of vertical results for 40% of filler

Vertical Results	Analysis
Position A	
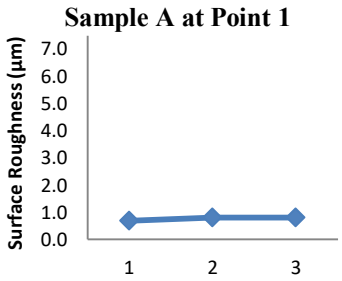	The value of surface roughness at this point is the highest for 40%of filler which they range up to 0.8 µm.
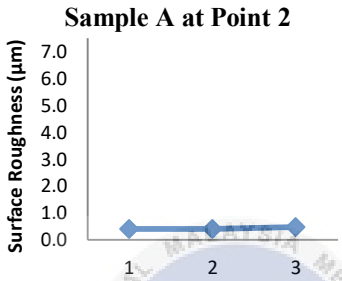	The graph shows there is small increasing of value at Reading 3 compared to two other remaining readings.
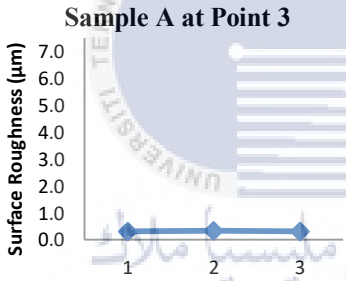	The data displays up to no difference among all of the three readings since their values are around 0.3 µm.
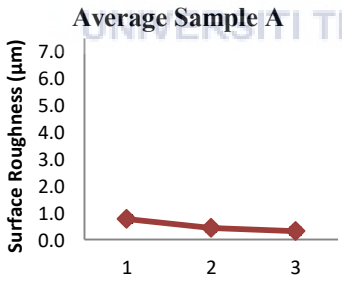	Ra value is the highest at point 1 but the average value starts decreasing at point 2 and point 3. The error bar is barely to see since the difference between the highest and the lowest value at each point is not exceeding over 0.12 µm.
Position B	
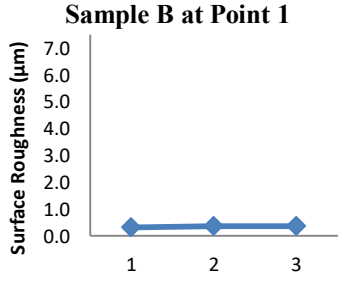	The value from the second and third readings shows consistency but differs from the value at Reading 1 that has lower value compared to the other two values.

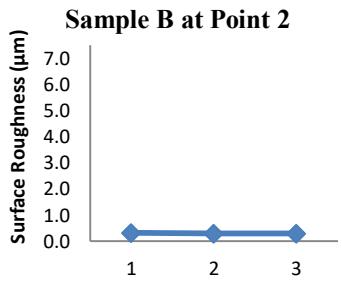	Graph displays consistency among all of the three readings led by the small difference in their value of surface roughness.
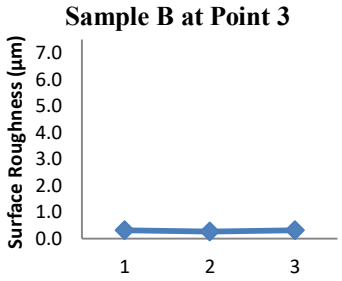	The graph illustrates that it has the lowest value of surface roughness for this sample that is in the range of 0.2 – 0.3 µm.
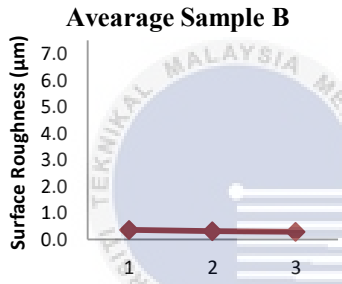	From the graph, the data shows consistency among the three readings which proves that there is up to no difference in Ra values. The error bar is barely to see which proves that there is small difference between the average values.
Total Average at Positions A & B	
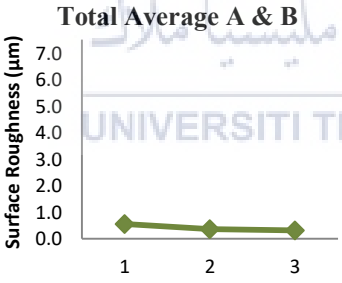	Total average values at point 2 and point 3 shows consistency but they are lower compared to the total value of Ra at the first point. The error bar is barely to see which explains that the total average values are more certain.

Table 4.12 Analysis of vertical results for 50% of filler

Vertical Results	Analysis
Position A	
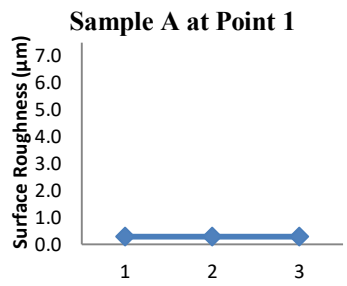	The graph exhibits a stable consistency among the values since the difference in their value of surface roughness is up to no difference at all.
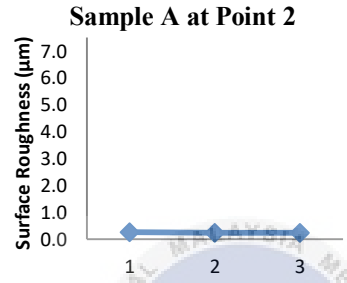	The graph also experiences the similar situation as in the previous graphs where the data being displayed has small difference.
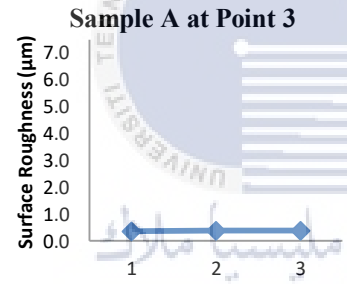	The values from Reading 1 and Reading 2 are consistent but at Reading 3, the value is slightly increasing.
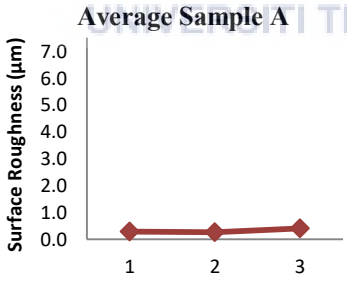	From Point 3, the increasing average value is obvious while the average values at Point 1 and Point 2 are consistent. The error bar is barely to see which caused by the difference between the highest and the lowest value at each point is only up to 0.03 µm.
Position B	
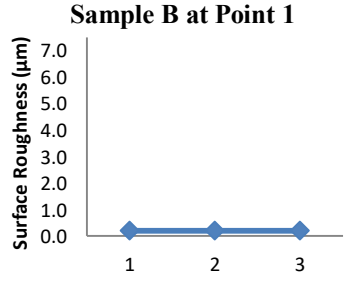	From this point, it has the lowest value surface roughness for 50% of filler and they exhibit the consistency in their values as can be seen in the graph.

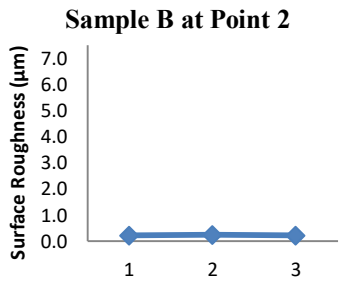	The graph also displays that the values of surface roughness at this point has stable consistency.
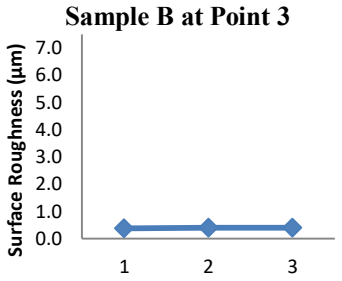	The graph illustrates that the values of surface roughness among all of three readings also have consistency.
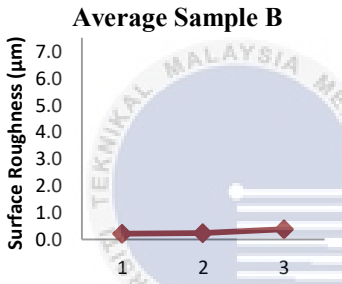	At Point 3, the average value is at its highest while the rests show small up to no difference in their average values. The error bar is barely to see due to the difference between the highest and the lowest value at each point is only maximized to 0.03 µm.
Total Average at Positions A & B	
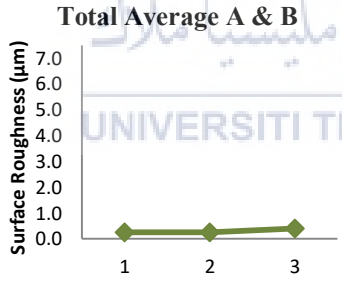	The total average values for all of three points have small difference but the total average at point 3 is a bit higher compared to other points. The error bar is barely to see which describes that the total average values are more certain.

Table 4.13 Analysis of vertical results for 60% of filler

Vertical Results	Analysis
Position A	
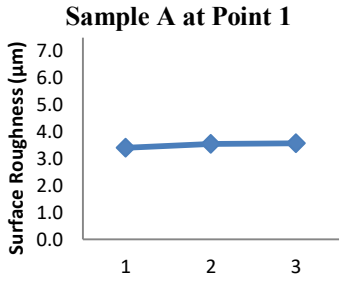	The values rapidly increasing from the previous percentage of fillers where they start from 2 µm and above. From the graph, the values at Reading 2 and Reading 3 are consistent while at Reading 1, the value is a bit lower.
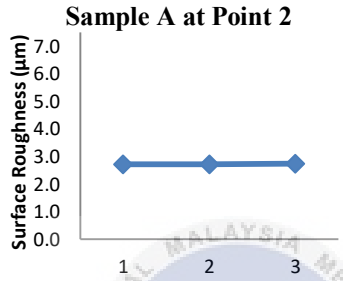	The graph displays stable consistency since their range is consistent that is around 2.7 µm.
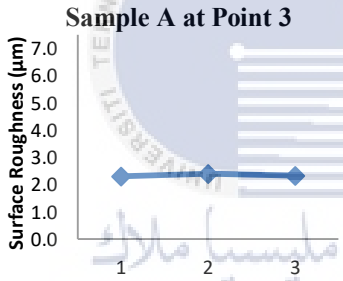	The value from Reading 2 is a bit higher compared to the values from Reading 1 and Reading 3 that are consistent between each other.
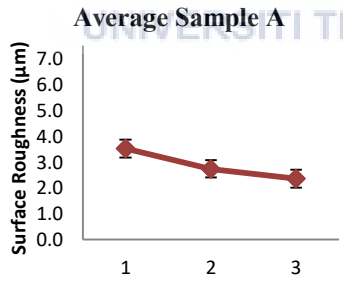	There is no stable consistency among the average values being displayed in the graph as the difference value between the highest and the lowest data is 1.16 µm. The error bar is in short length due to difference between the highest and the lowest value at each point are 0.138 µm, 0.036 µm and 0.107 µm.
Position B	
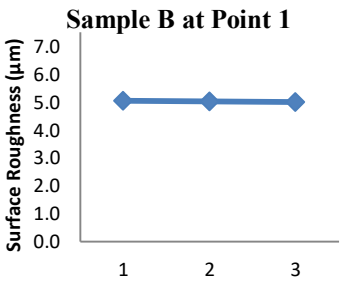	The graph exhibits consistency in the data but the value from Reading 3 is slightly lower than the other values.

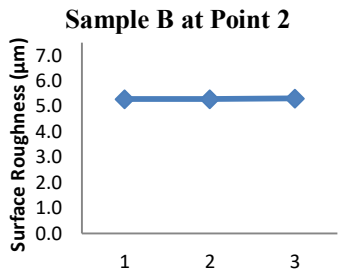	At this point, the value of surface roughness is the highest for this sample with the range or 5.2 – 5.3 µm.
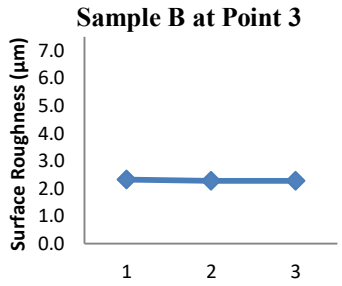	It has the lowest value of surface roughness for 60 % of filler that is in the range of 2.3 – 2.8 µm while the data shows consistency in their value.
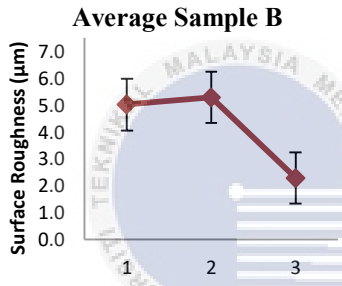	The average values at point 1 and point 2 has small difference but the value drops rapidly at point 3 as can be seen in the graph. The error bars show long dimension which means that the concentration of average values was calculated on is low.
Total Average at Positions A & B	
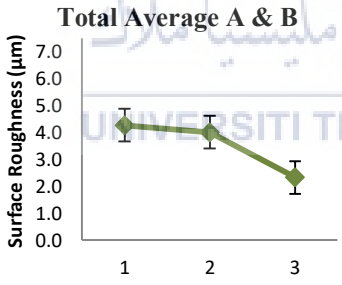	The total average value at point 3 has big gap compared to the values at point 1 and point 2 as it experiences high decreasing of value. The error bar displays big difference which means that the total average values of surface roughness is uncertain.

Table 4.14 Analysis of vertical results for 70% of filler

Vertical Results	Analysis
Position A	
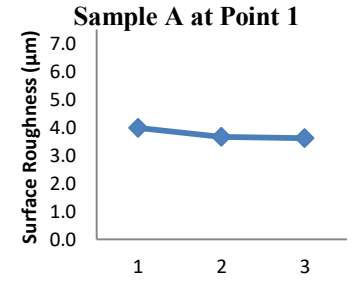	From Reading 1, the surface roughness value is the highest while the other values at Reading 2 and Reading 3 has small gap between each other which leads to consistency.
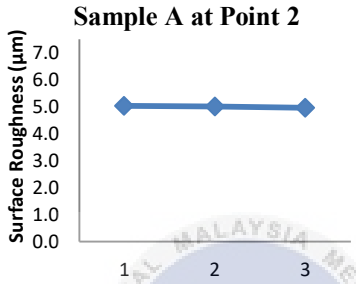	The data produces a consistent graph plot since there is small gap between all of the surface roughness values.
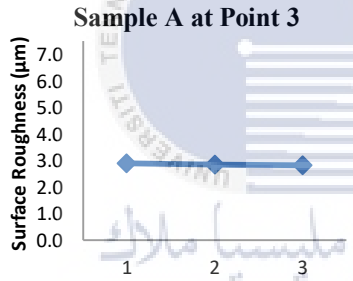	From the graph, it shows that the values are consistent as all of the values start from 2.8 µm.
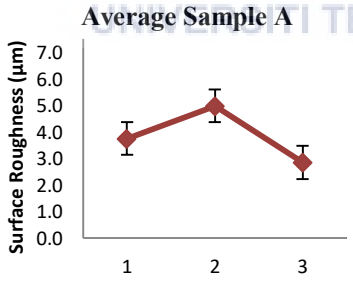	The graph displays irregular consistency as the gap between each of the average value is large. The average value at point 2 is the highest being compared to the other points. The error bar displays big difference which also means the average values of surface roughness is uncertain.
Position B	
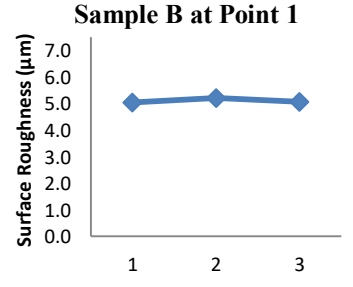	The surface roughness values from Reading 2 and Reading 3 has small difference while the value from the first reading is the lowest for this point.

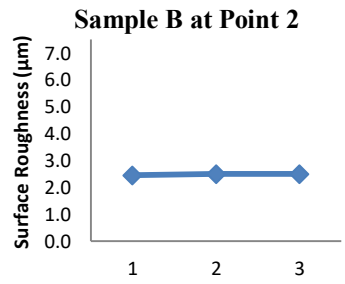	Graph has the lowest surface roughness value for 70% of filler and the value from Reading 1 is the lowest while the values at Reading 2 and Reading 3 being consistent.
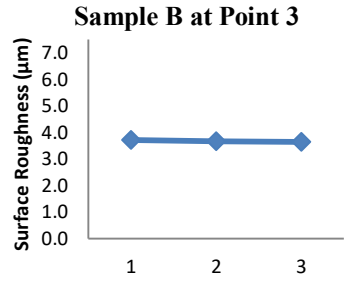	The data produces a consistent graph plot since there is small gap between all of the surface roughness values.
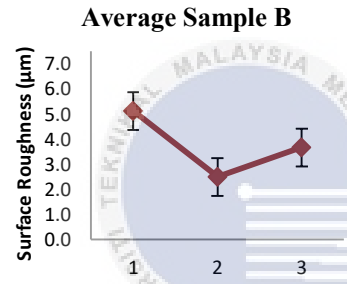	The graph exhibits irregular consistency as the gap between each of the average value is large. The average value at point 2 is the lowest being compared to the other points. The error bars show long dimension which means that the concentration of average values was calculated on is low.
Total Average at Positions A & B	
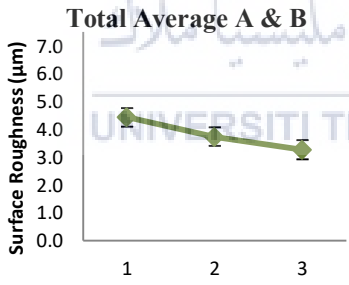	The total average values are gradually decreasing across all of three points which indicates the presence of irregular consistency. The error bar appears to be small that means the total average values of surface irregularities on the sample are slightly certain.

Table 4.15 Analysis of vertical results for 80% of filler

Vertical Results	Analysis
Position A	
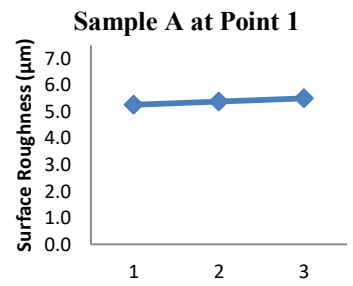	Through the graph, the data can be seen gradually increases across all of the readings with small gap between each readings.
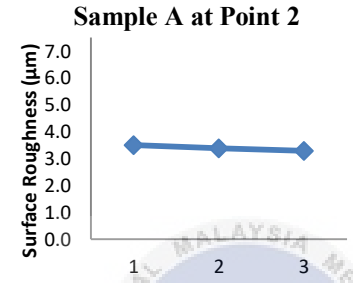	The surface roughness values from Reading 2 and Reading 3 produce consistent graph plot while the value at Reading1 is slightly the highest at this point.
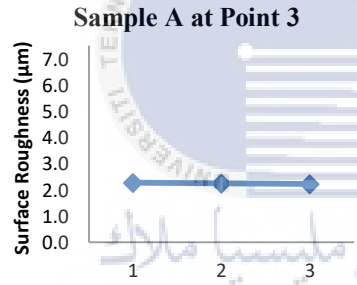	The graph exhibits consistency between all of the values of surface roughness across all of the readings.
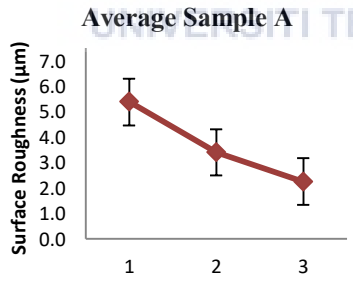	Ra is gradually decreasing across all of three points which indicates the presence of irregular consistency. The error bar appears to be large caused by the concentration of average values was calculated on is low plus the difference between the highest and the lowest average value is high, 2.13 µm.
Position B	
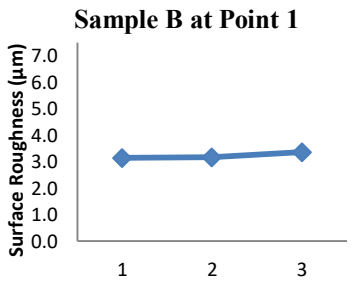	At Reading 1 and Reading 2, the data shows consistency but the data increases from Reading 3 which shows there is obvious gap between the values from Reading 2 and Reading 3.

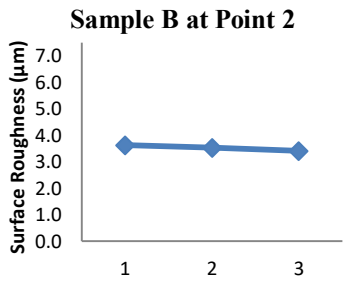	From the graph, the surface roughness value at Reading 1 is the highest and the values gradually decrease across all of the readings with small difference.
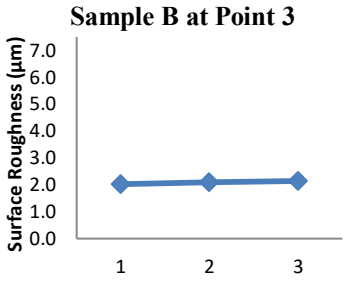	The surface roughness value at Reading 3 is the highest compared to other two points that have small difference in value between each other.
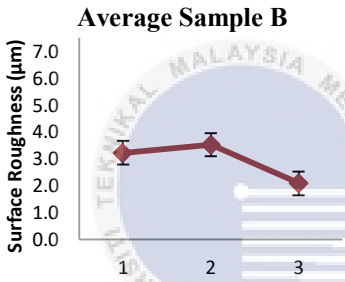	The graph displays irregular consistency as the difference between each of the value is large. The average value at point 3 is the lowest being compared to the other points. The error bar appears to be short that means the average values surface irregularities on the sample are slightly certain.
Total Average at Positions A & B	
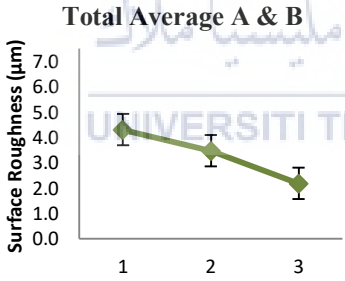	The total average values are gradually decreasing across the points with the range of gap 0.8 – 1.3 µm. The error bar appears to be large that means the total average values of surface irregularities is uncertain.

Table 4.16 Analysis of vertical results for 90% of filler

Vertical Results	Analysis
Position A	
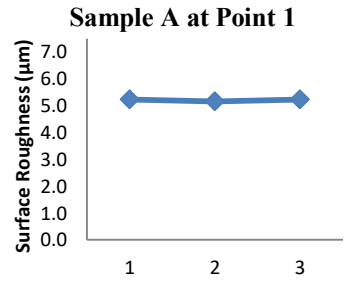	The surface roughness values from Reading 1 and Reading 3 are consistent while the value at Reading 2 is a bit decreasing.
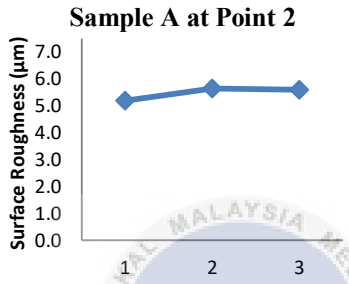	Graph shows that the surface roughness values from Reading 2 and Reading 3 are consistent while the value at Reading 1 has obvious difference from the other values.
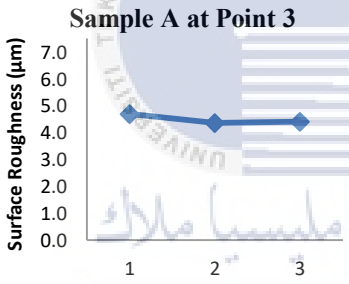	From the graph, the surface roughness value at Reading 1 is the highest while the values from Reading 2 and Reading 3 displays stable consistency.
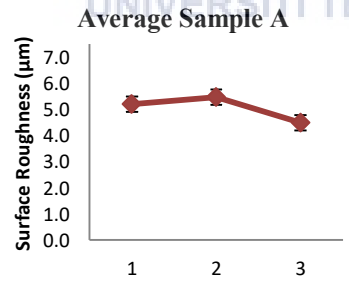	Each of average values has small difference between all of the points and the average value at point 2 being the highest value. The error bar appears to be small that means the surface irregularities on the sample are slightly consistent.
Position B	
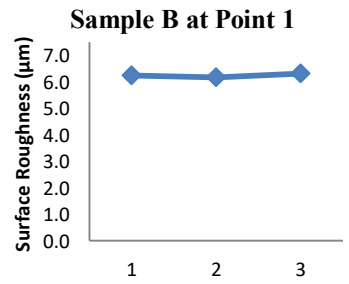	The total Ra values from Reading 1 and Reading 3 exhibits consistency while the value at Reading 2 being the lowest among them.

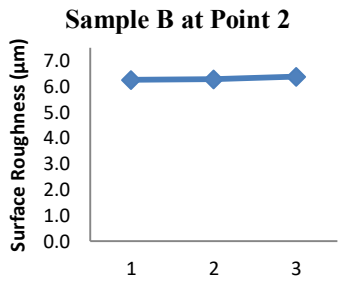	From the graph, the surface roughness values from Reading 3 shows the highest value of surface roughness while at Reading 1 and Reading 2, their values are consistent
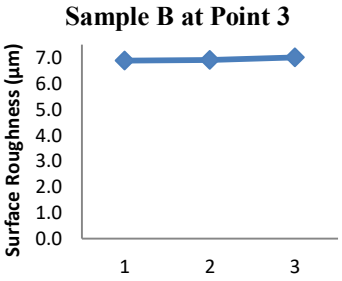	The Ra values from Reading 1 and Reading 2 are consistent while at Reading 3, it shows the highest value of surface roughness.
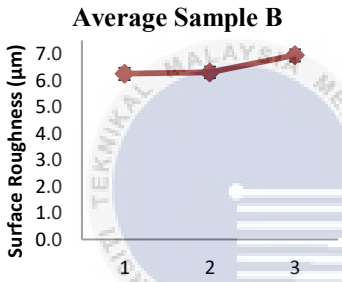	The average values at point 1 and point 2 show consistency while the average values at point 3 being the highest among all of the points. The error bar appears to be small that means the surface irregularities on the sample are slightly certain.
Total Average at Positions A & B	
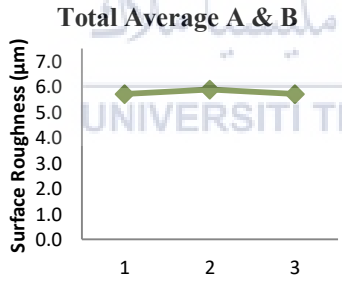	From the graph, it shows that the total Ra values at each point have small difference between each other. The error bar is hardly to see which explains that there is slightly small difference between the total average values and the concentration of average values was calculated on is high.

4.4.2 Surface roughness in horizontal direction

Each of the data is translated into the graph that represents three types of relation; relationship between surface roughness and number of measurement taken on the same spot, relationship between Ra and point of measurement and relationship between total Ra and measurement points at both positions.

Table 4.17 Horizontal results

% of Filler	Position	Surface Roughness (μm)								
		Point 1	Average	Total Average A & B	Point 2	Average	Total Average A & B	Point 3	Average	Total Average A & B
10	A	0.202	0.189	0.215	0.189	0.190	0.228	0.115	0.121	0.121
		0.181			0.170			0.124		
		0.184			0.212			0.125		
	B	0.256	0.241		0.277	0.266		0.120	0.120	
		0.235			0.258			0.121		
		0.233			0.264			0.118		
20	A	0.828	0.830	0.943	1.450	1.450	1.507	1.116	1.116	1.135
		0.825			1.454			1.122		
		0.836			1.445			1.111		
	B	1.058	1.056		1.554	1.565		1.151	1.154	
		1.052			1.572			1.161		
		1.059			1.569			1.149		
30	A	1.288	1.327	0.952	1.597	1.568	1.506	1.155	1.149	1.116
		1.343			1.603			1.136		
		1.349			1.503			1.155		
	B	0.586	0.578		1.439	1.444		1.078	1.084	
		0.575			1.436			1.092		
		0.572			1.456			1.082		
40	A	0.493	0.497	0.469	0.222	0.221	0.228	0.336	0.339	0.340
		0.496			0.218			0.349		
		0.501			0.224			0.333		
	B	0.437	0.441		0.230	0.234		0.337	0.340	
		0.444			0.239			0.339		
		0.441			0.234			0.343		
50	A	0.385	0.373	0.502	0.458	0.463	0.439	1.587	1.595	1.071
		0.367			0.459			1.606		
		0.366			0.473			1.591		
	B	0.754	0.631		0.367	0.415		0.530	0.547	
		0.539			0.405			0.556		
		0.601			0.472			0.554		
60	A	4.108	4.185	4.238	3.228	3.218	3.546	2.840	2.774	3.186
		4.213			3.209			2.713		
		4.235			3.218			2.769		
	B	4.299	4.291		3.865	3.873		3.592	3.597	
		4.314			3.887			3.596		
		4.261			3.866			3.604		
70	A	3.502	3.510	3.516	4.666	4.686	4.393	4.428	4.464	4.132
		3.507			4.691			4.491		
		3.521			4.700			4.473		
	B	3.535	3.523		4.091	4.101		3.735	3.800	
		3.531			4.117			3.744		
		3.502			4.095			3.920		
80	A	5.266	5.287	4.335	3.212	3.215	3.366	3.849	3.859	3.740
		5.226			3.221			3.855		
		5.370			3.213			3.873		
	B	3.409	3.382		3.541	3.516		3.628	3.621	
		3.349			3.509			3.620		
		3.387			3.499			3.614		
90	A	4.288	4.194	4.765	4.948	5.076	5.279	5.018	5.026	5.641
		4.212			5.166			5.151		
		4.083			5.114			4.910		
	B	5.288	5.335		5.465	5.483		6.240	6.255	
		5.335			5.493			6.248		
		5.382			5.490			6.276		

Table 4.18 Analysis of horizontal results for 10% of filler

Horizontal Results	Analysis
Position A	
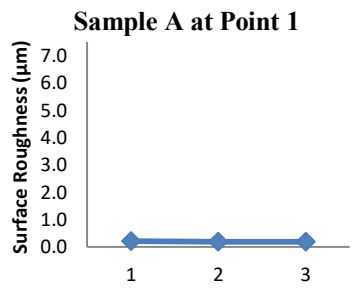	Graph has low surface roughness that is in range of 0.18 – 0.25 µm, which means that the result has stable consistency.
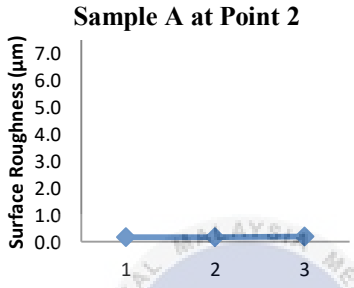	The graph illustrates low surface roughness where the range is 0.18 – 0.25 µm, similarly to the previous point.
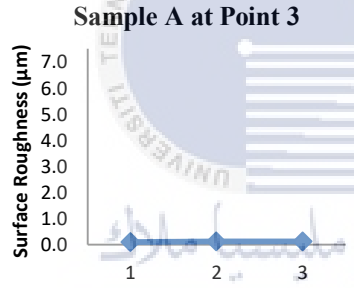	This area has the lowest surface roughness that is in range of 0 – 0.15 µm, which means that it has the smoothest surface.
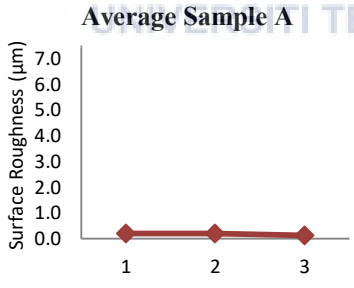	At point 3, Ra between three points is the lowest compared to the other two points, but the sample still has smooth surface. The error bar appears to be short since the difference between the highest and the lowest values at each point are 0.021 µm, 0.042 µm and 0.010 µm
Position B	
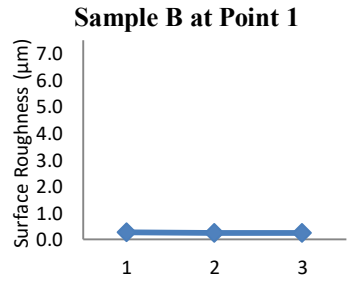	The graph illustrates low surface roughness with small gap of value between the times of data reading.

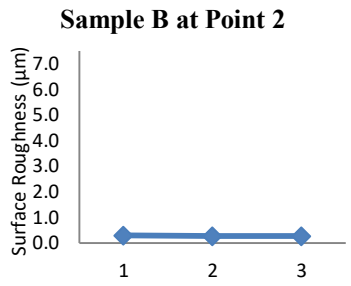	Graph has the highest surface roughness value compared to other points in both position, but in consistent range.
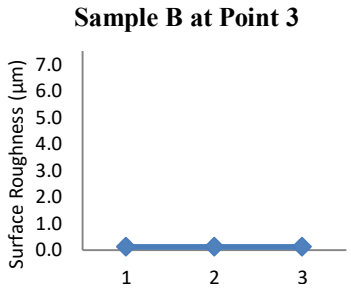	Graph has the lowest surface roughness value compared to the value in this position. At third reading when the data is taken, the value slightly decreases.
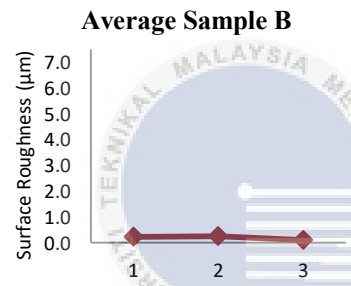	At the first and second points the data is taken, the Ra value is consistent while at the third point, the value decreases, but the sample is still in homogenous solution since the value gap is small. The error bar is barely to see since the difference between the highest and the lowest value at each point is not exceeding over 0.03 µm.
Total Average at Positions A & B	
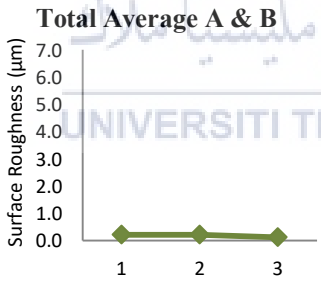	At point 1 and 2, the total Ra is consistent while at point 3, it decreases in value but in small gap, which describes that the sample is in homogenous solution. The error bar is barely to see which proves that the total average values are more certain.

Table 4.19 Analysis of horizontal results for 20% of filler

Horizontal Results	Analysis
Position A	
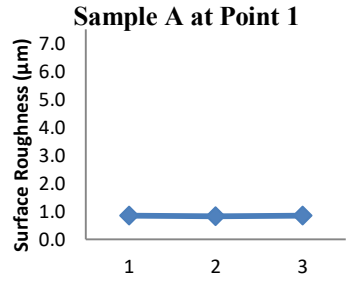	This area has the lowest surface roughness that is in range of 0.5 – 1 µm, which means that it has the smoothest surface.
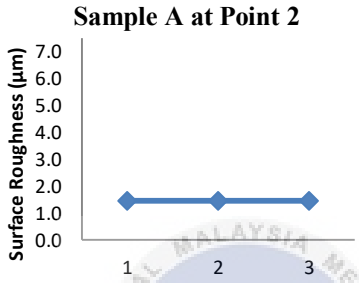	Graph consists of range of surface roughness around 1.45 µm with consistent gap, which is the highest in this position. Ra value rapidly increases compared to the previous point.
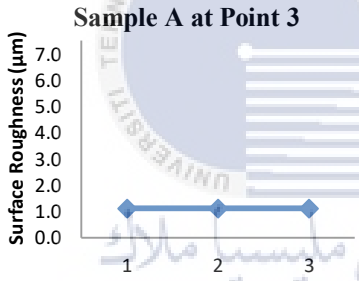	This area has lower surface roughness compared to the data at Point 2 with small gap between each data that proves the result has stable consistency.
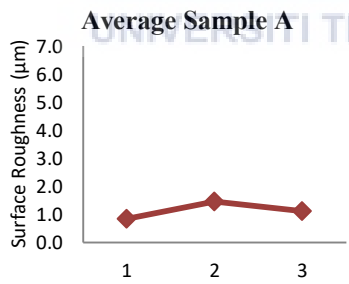	At point 1, the Ra between three points is the lowest compared to the other two points, but the sample still has smooth surface. The error bar is barely to se that means the surface irregularities on the sample are slightly consistent.
Position B	
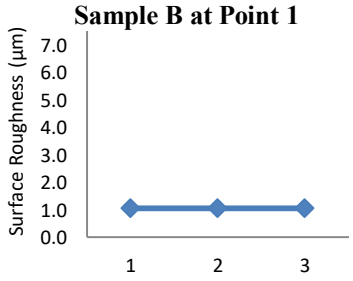	It has the lowest surface roughness value compared to the value in this position with small gap of value between the times of data reading.

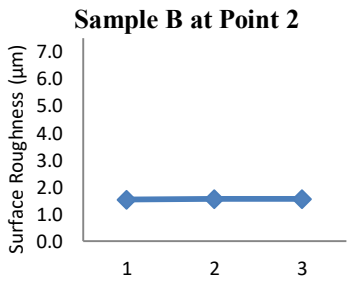	It has the highest surface roughness value compared to other points in both position, but in consistent range.
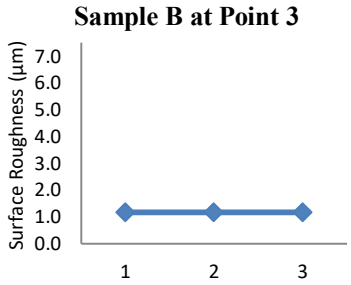	The graph illustrates low surface roughness but at third reading when the data is taken, the value slightly increases.
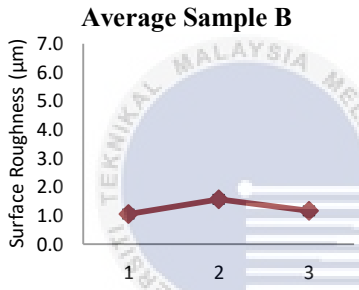	At the second points the data is taken, the average value is the highest while at the rest of two points point; the value decreases, but the sample is still in homogenous solution since the value gap is small. The error bar appears to be small due to the data distribution consistently starts from 1.0 µm until 1.6 µm only.
Total Average at Positions A & B	
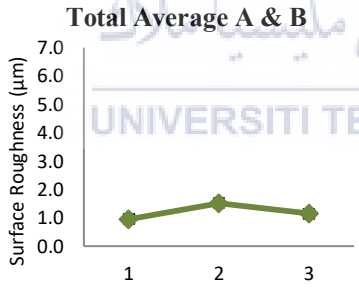	At point 2 and 3, the total Ra in the range of 1.1 -1.6 µm while at point 1, it decreases in value but in small gap, which describes that the sample is in homogenous solution. The error bar is barely to see which proves that the total average values are more certain.

Table 4.20 Analysis of horizontal results for 30% of filler

Horizontal Results	Analysis
Position A	
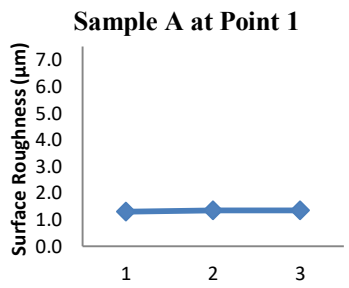	It has surface roughness that is in range of 1.28 – 1.35 µm, which means that the result has stable consistency as it has small gap between the data.
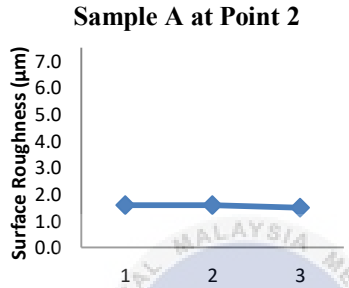	The graph illustrates low surface roughness where the range is 1.5 – 1.6 µm, but it increases compared to the previous point.
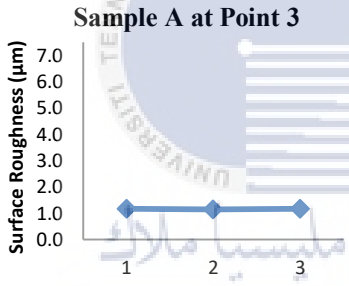	This area has the lowest surface roughness that is in range of 1.13 – 1.16 µm, which means that it still has the smoothest surface.
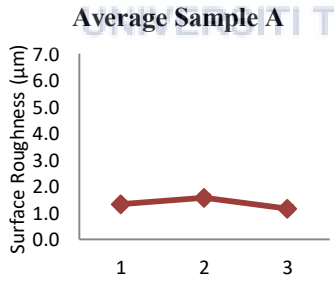	At point 3, the average of surface roughness between three points is the lowest compared to the other two points, but the sample still has smooth surface. The error bar appears to be small due to the data distribution consistently starts in the range of 1.13 µm until 1.61 µm.
Position B	
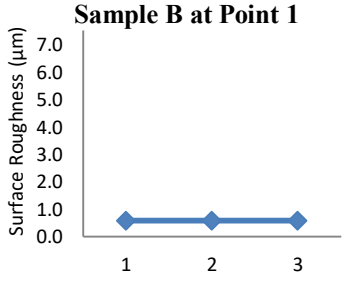	It has the lowest surface roughness value compared to other points in both position, but in consistent range.

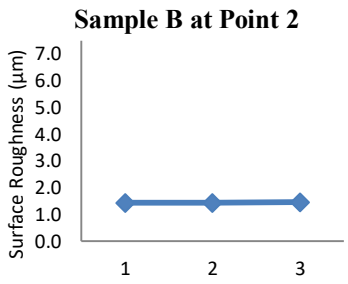	It has the highest surface roughness value compared to the value in this position with very few gap between the data.
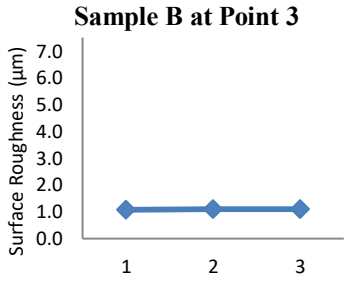	The graph illustrates low surface roughness with small gap of value between the times of data reading.
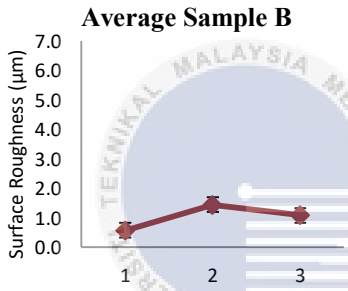	At the second and third points the data is taken, the average value has a difference of 0.36 µm while at the first point, the value decreases, but the sample is still in homogenous solution since the value gap is small. The error bar appears to be short since the difference between the highest and the lowest values at each point are small; 0.014 µm, 0.002 µm and 0.014 µm.
Total Average at Positions A & B	
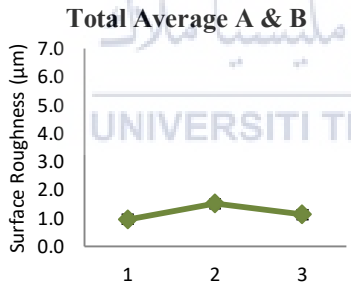	At point 2 and 3, the total Ra value has small difference while at point 1; it decreases in value but in small gap, which describes that the sample is still in homogenous solution. The error bar is barely to see which means that the concentration of average values was calculated on is high.

Table 4.21 Analysis of horizontal results for 40% of filler

Horizontal Results	Analysis
Position A	
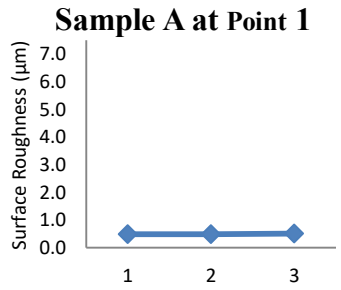	The value of surface roughness at this point is the highest for 40% of filler which they range up to 0.5 µm.
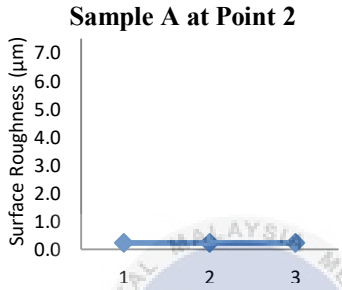	The graph exhibits there is small increasing of value at Reading 3 compared to two other remaining readings.
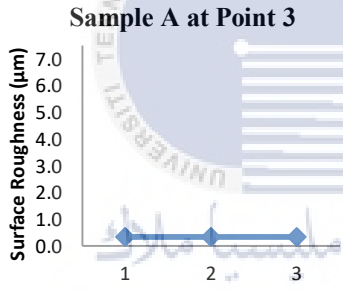	The data presents up to no difference among all of the three readings since their values are around 0.3 µm.
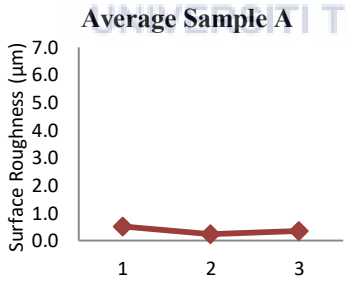	The average value of surface roughness is the highest at point 1 but the average value starts decreasing at point 2 and point 3. The error bar is hardly to see which proves that there is small difference between the average values.
Position B	
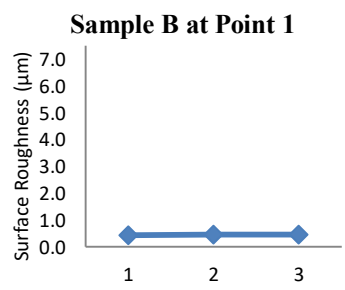	Highest surface roughness with small gap of value between the times of data reading.

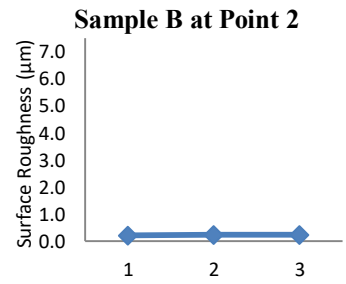	Graph displays consistency among all of the three readings led by the small difference in their value of surface roughness.
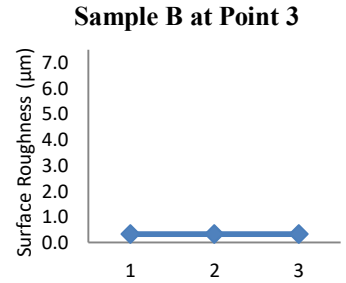	It has the lowest surface roughness value compared to other values in this position.
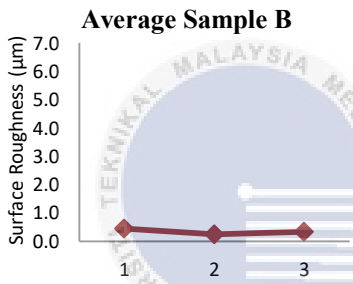	The average value at points 2 and 3 is consistent while at the first point, the value is a bit higher, but the sample is still in homogenous solution since the value gap is small. The error bar appears to be small that means the surface irregularities on the sample are slightly consistent.
Total Average at Positions A & B	
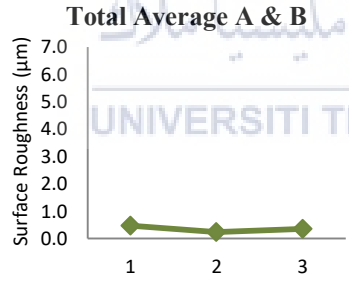	The total Ra values at point 2 and point 3 shows consistency but they are lower compared to the total Ra value of surface roughness at the first point. The error bar is hardly to see which means that the concentration of average values was calculated on is high.

Table 4.22 Analysis of horizontal results for 50% of filler

Horizontal Results	Analysis
Position A	
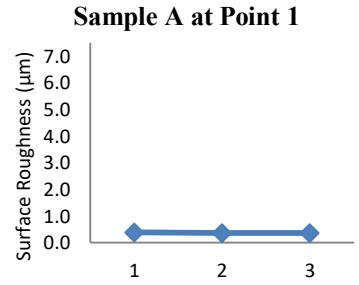	The graph shows a stable consistency among the values since the difference in their value of surface roughness is up to none difference.
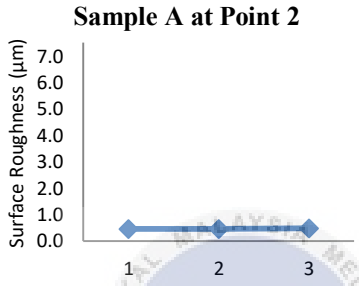	The graph also encounters similar situation as in the previous graphs where the data being displayed has small difference.
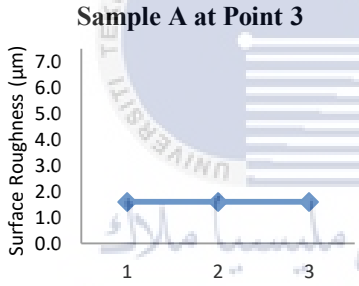	The values from Reading 1 and Reading 2 are consistent but at Reading 3, the value is slightly increasing.
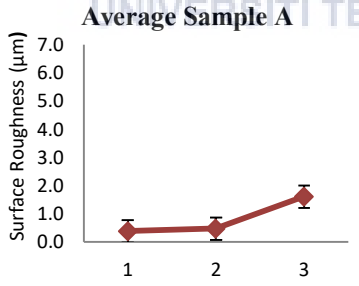	From Point 3, the increasing average value is obvious while the average values at Point 1 and Point 2 are consistent. The error bar appears to be obvious as the difference between the highest and the lowest values at each point are small; 0.019 µm, 0.015 µm and 0.015 µm
Position B	
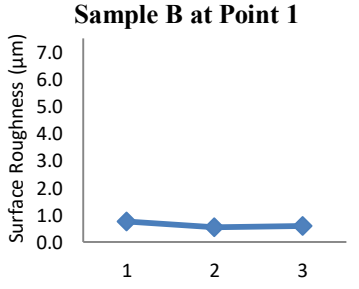	From the graph, the surface roughness value at Reading 1 is the highest while the values from Reading 2 and Reading 3 displays stable consistency.

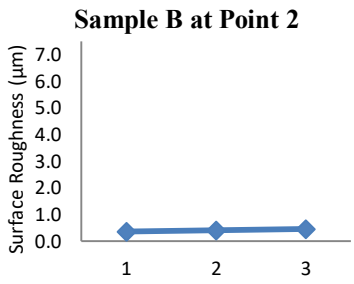	From this point, it has the lowest value surface roughness in this position and they exhibit an increasing value at point 3 as can be seen in the graph.
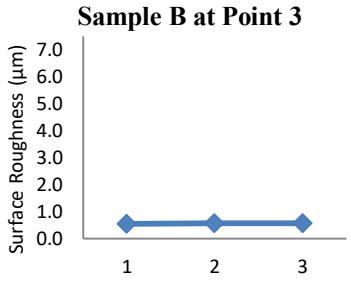	The graph displays consistency between all of the values of surface roughness across all of the readings.
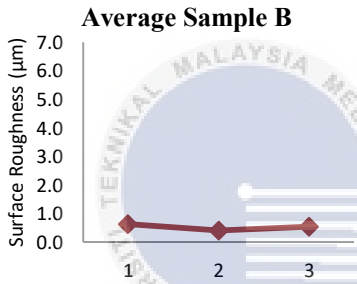	At the second and third points the data is taken, the average value is consistent while at Point 1, the value is a bit higher, but the sample is still in homogenous solution since the value gap is small. The error bar is barely to see due to the difference between the highest and the lowest value at each point is only maximized to 0.2 µm.
Total Average at Positions A & B	
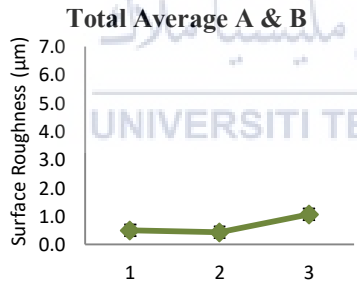	At point 1 and 2, the total average of surface roughness is consistent while at point 3, it increases in value with big gap. The error bar is small which proves that the concentration of total average values was calculated on is high.

Table 4.23 Analysis of horizontal results for 60% of filler

Horizontal Results	Analysis
Position A	
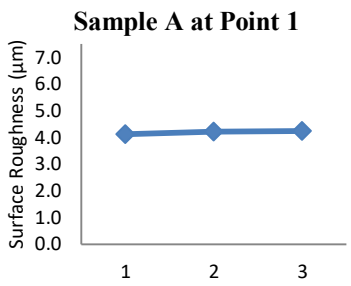	The values rapidly increasing from the previous percentage of fillers where they start from 2 µm and above.
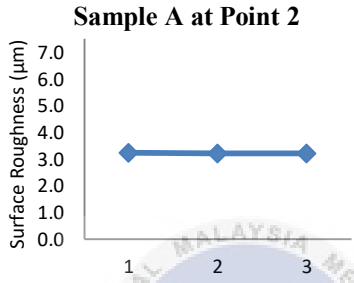	The graph displays stable consistency since their range is consistent that is around 3.2 µm.
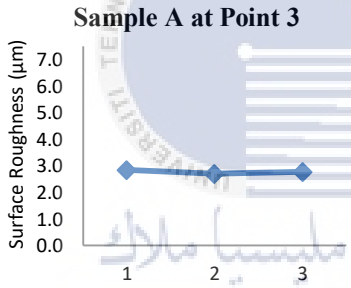	The value from Reading 1 is a bit higher compared to the values from Reading 2 and Reading 3 that are consistent between each other.
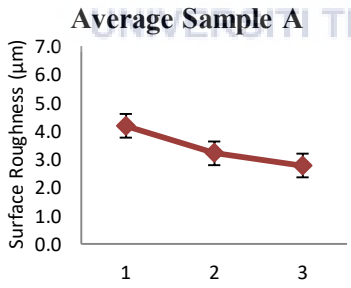	There is no stable consistency among the average values being displayed in the graph as the difference value between the highest and the lowest data is 1.411 µm. The error bar is in obvious dimension since the difference between the highest and the lowest values at each point are 0.127 µm, 0.019 µm and 0.127 µm
Position B	
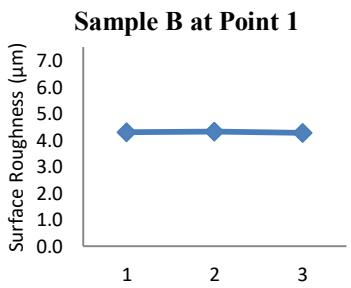	The graph exhibits consistency in the data but the value from Reading 3 is slightly lower than the other values.

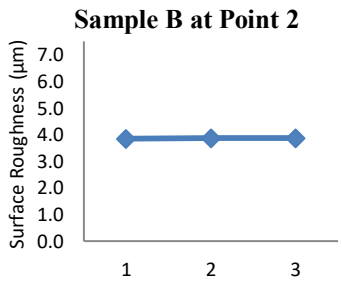	The graph shows a stable consistency among the values since the difference in their value of surface roughness is up to no difference at all.
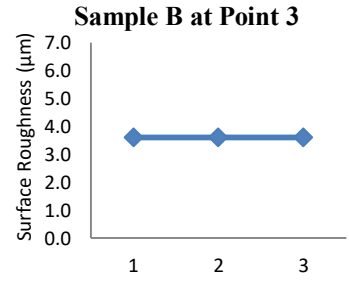	It has the lowest surface roughness value compared to the value in this position. At third reading when the data is taken, the value is slightly increases.
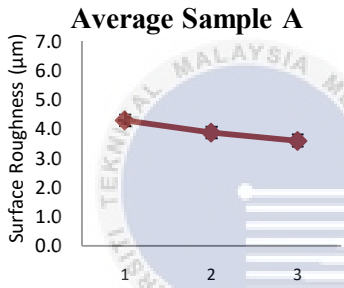	The average value gradually decreases; the error bar appears to be small that means the surface irregularities on the sample are slightly consistent.
Total Average at Positions A & B	
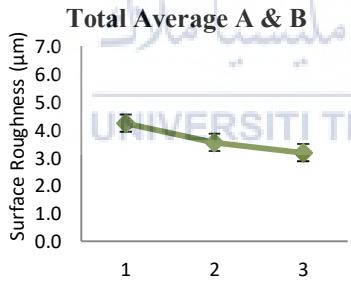	The total average values are gradually decreasing across all of three points which indicates the presence of irregular consistency. The error bar appears to be small that means the total average surface irregularities on the sample are slightly consistent.

Table 4.24 Analysis of horizontal results for 70% of filler

Horizontal Results	Analysis
Position A	
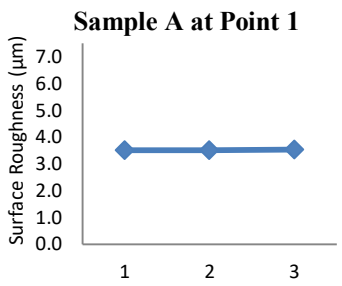	From the graph, it shows that the values are consistent as all of the values start from 3.5 µm.
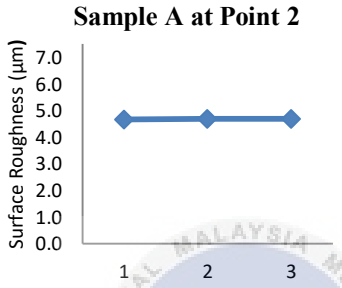	Data distribution does not produce obvious inconsistency in the graph as the gap between each data is small.
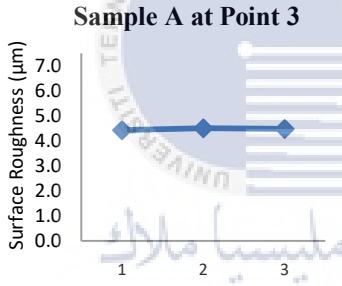	The data produces a consistent graph plot since there is small gap between all of the surface roughness values.
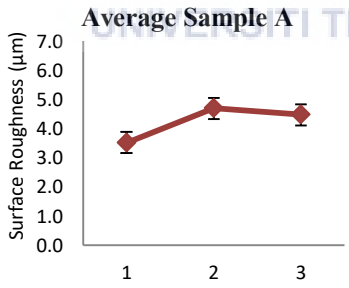	The graph displays irregular consistency as the difference between each of the average value is large. The average value at point 1 is the lowest being compared to the other points. The error bar appears to be small caused by the concentration of Ra values was calculated on is high plus the difference between the highest and the lowest average value is low, 0.954 µm.
Position B	
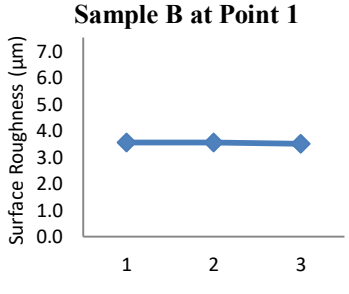	It has the lowest surface roughness value compared to the value in this position. At third reading when the data is taken, the value slightly increases.

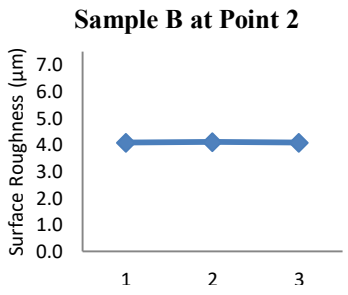	It has the highest surface roughness value compared to other points in both position, but in consistent range.
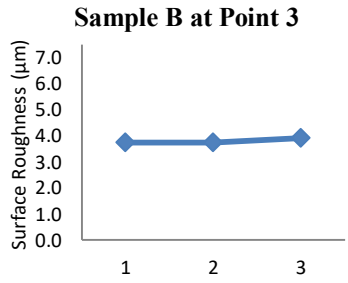	From the graph, the surface roughness value at Reading 1 is the lowest and the values gradually increase across all of the readings with small difference.
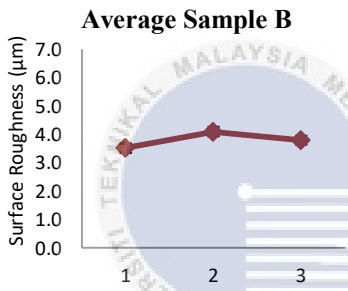	The graph displays irregular consistency as the difference between each of the average value is large. The average value at point 1 is the lowest being compared to the other points. The error bar appears hardly to see that means the surface irregularities on the sample are slightly consistent.
Total Average at Positions A & B	
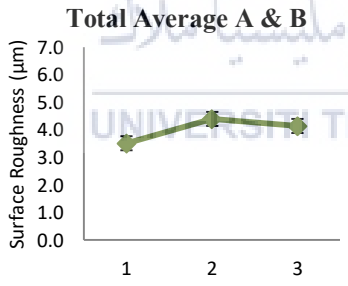	The total average value at point 1 has big gap compared to the values at point 2 and point 3 as it experiences high decreasing of value. The error bar is barely to see caused by the concentration of total average values was calculated on is high.

Table 4.25 Analysis of horizontal results for 80% of filler

Horizontal Results	Analysis
Position A	
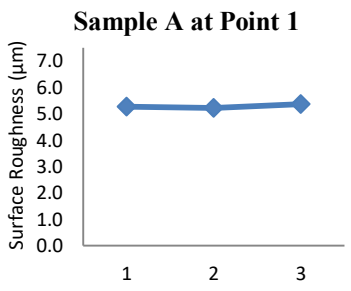	The values from Reading 1 and Reading 2 are consistent but at Reading 3, the value is slightly increasing.
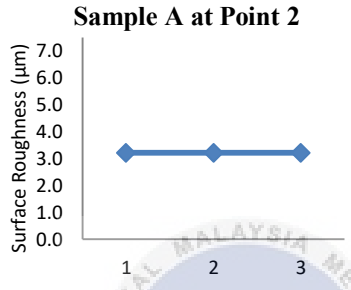	It has the lowest surface roughness value compared to the value in this position. At second reading when the data is taken, the value slightly increases.
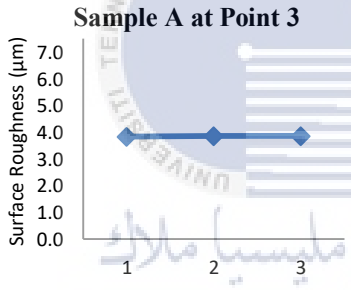	The graph shows stable consistency since their range is consistent that is around 3.8 µm.
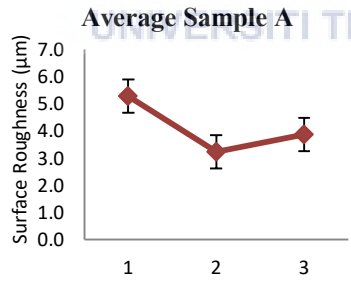	The graph exhibits irregular consistency as the gap between each of the average value is large. The average value at point 2 is the lowest being compared to the other points. The error bar appears to be large caused by the concentration of average values was calculated on is low plus the difference between the highest and the lowest average value is high, 2.072 µm.
Position B	
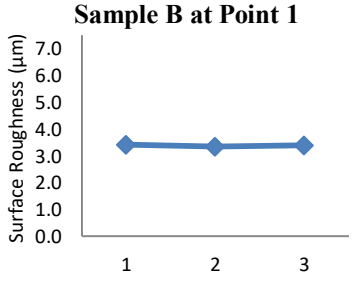	The surface roughness values from Reading 1 and Reading 3 has small difference while the value from the second reading is the lowest for this point.

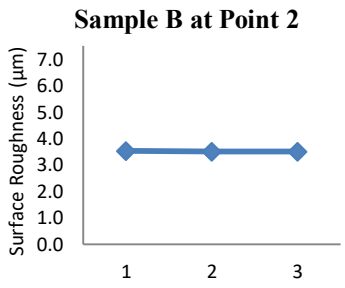	The data produces a consistent graph plot since there is small gap between all of the surface roughness values.
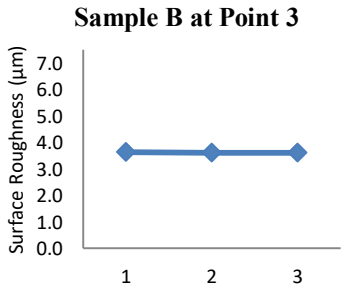	The graph shows a stable consistency among the values since the difference in their value of surface roughness is up to none difference.
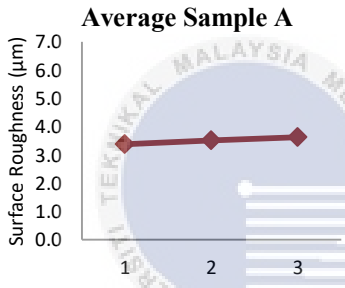	The average value gradually increases; the error bar appears barely to see that means the surface irregularities on the sample are certain.
Total Average at Positions A & B	
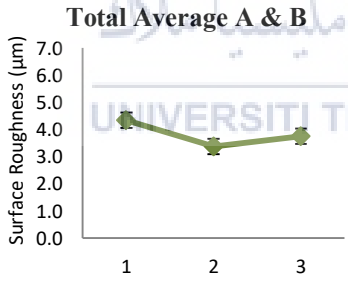	From the graph; at point 2 and 3, the total average value has small difference while at point 1; it has the highest value but in small gap. The error bar appears to be small since the difference between the highest and the lowest total average value is below 1 µm.

Table 4.26 Analysis of horizontal results for 90% of filler

Horizontal Results	Analysis
Position A	
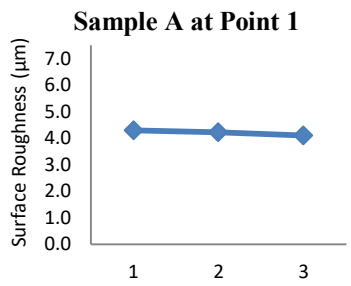	The surface roughness values from Reading 1 and Reading 2 produce consistent graph plot while the value at Reading 3 is slightly lower at this point.
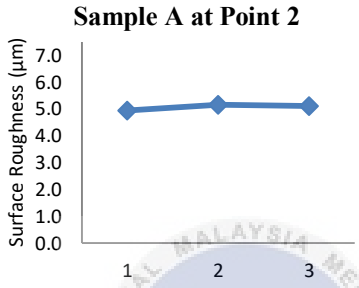	The values rapidly increasing from the previous percentage of fillers where they start from 5 µm and above. From the graph, the values at Reading 2 and Reading 3 are consistent while at Reading 1, the value is a bit lower.
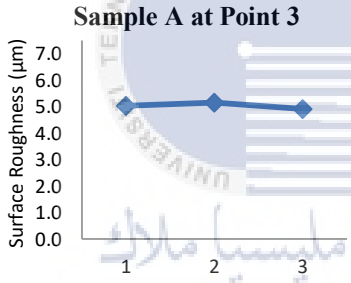	The value from Reading 3 is the lowest compared to the values from Reading 1 and Reading 3 that have small gap between each other.
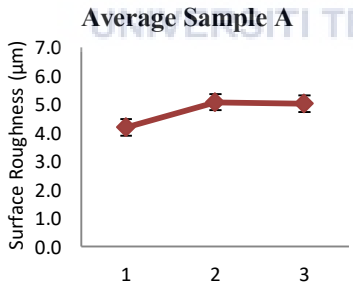	Through the graph, Ra starts to increase from Reading 1 to Reading 2 with the difference value of 0.882 µm while the data keeps consistent between the second and third readings. The error bar is in small dimension that is caused by the difference between the highest and the lowest value at each point is only up to 0.25 µm.
Position B	
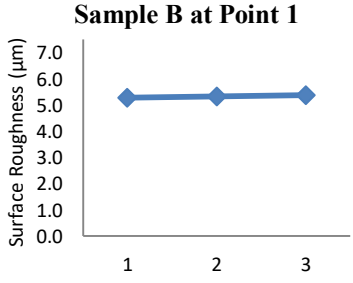	The graph displays consistency between all of the values of surface roughness across all of the readings with slight increase at Reading 3.

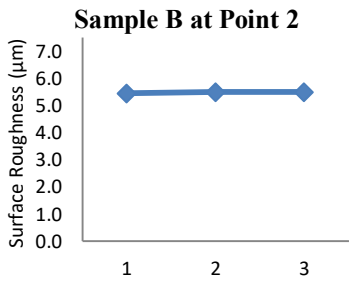	From the graph, it shows that the values are consistent as all of the values start from 5.4 µm.
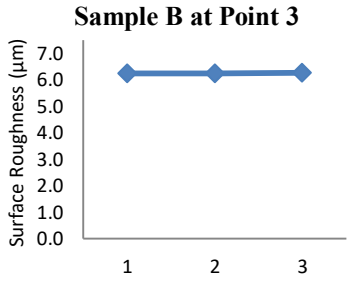	It has the highest surface roughness value for 90% of filler and the value keeps in stable consistency as their values start from 6.2 µm and above.
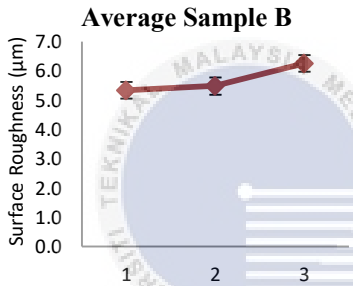	Average values from points 1 and 2 have small difference but the average value at point 3 increases thus, being the highest value. The error bar appears to be short due to the difference between the highest and the lowest value at each point is only maximized to 0.042 µm.
Total Average at Positions A & B	
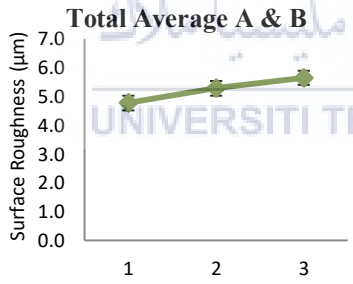	Total Ra value keeps increasing across the three points as shown in the graph. The error bar appears to be small that means the total average values of surface irregularities on the sample are certain and the concentration of average values was calculated on is high.

4.4.3 Critical discussion in vertical and horizontal directions

From the table of results in both directions, the values of surface roughness for the sample of 10% of filler until 50% of filler were below 1.9 µm with the lowest value of Ra in vertical direction was 0.091 µm while in horizontal direction was 0.115 µm. The highest value of Ra from 10% of filler until 50% of filler in vertical direction was 1.803 µm and for the horizontal direction; the highest Ra value was 1.606 µm.

For 60% of filler till the rests of the sample, their values of surface roughness in both directions surpassed 2.0 µm with the highest value of Ra was 7.017 µm in vertical direction and 6.276 µm in horizontal direction.

In vertical direction, graph that showed the stable consistency was resulted from 10% of filler up to 50% of filler including 90% of filler, and the graph with the most stable consistency was exhibited from the graph of 50% of filler since there was no much difference between the data taken. The rests of the sample from 60% - 80% of filler displayed irregular consistency among the recorded data from the large error detected in the graph that indicating the concentration of average values was calculated is low, thus that the average value was uncertain.

For horizontal direction, graph that illustrated the stable consistency was contributed from 10% - 70% of filler including 90% of filler since their error bar from the graph of average values and total values of Ra was small or barely to see which proved that the concentration of average values was calculated is high, thus that the average value was certain. Graph of average and total average values of Ra at 80% of filler displayed the most obvious difference in the error bar as the error bar was long which means that the surface irregularities on the sample were not consistent.

From all of the graphs that had been constructed, they attributed that the samples with lower filler percentage had consistent Ra and smooth surface. Meanwhile, for the samples with high percentage of filler had inconsistent surface irregularities that contributed to rougher surface.

4.5 RELATIONSHIP BETWEEN ELECTRICAL PROPERTIES, MORPHOLOGICAL AND SURFACE ROUGHNESS

Table 4.27 Resistivity versus Surface Roughness versus Microstructure

Filler (%)	Binder (%)	Point	Resistivity (Ω/sq)	Surface Roughness (µm)		Microstructure (Magnification of 20x)
			Total Average at Positions A & B	Total Average at Positions A & B		
				Horizontal Direction	Vertical Direction	
10	90	1	-	0.215	0.281	Dark spot was presumed as AgNPs 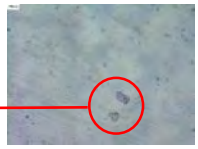
		2		0.228	0.276	
		3		0.121	0.114	
20	80	1	-	0.943	0.689	Dark spot was presumed as AgNPs 
		2		1.507	0.229	
		3		1.135	0.111	
30	70	1	-	0.952	0.686	Dark spot was presumed as AgNPs 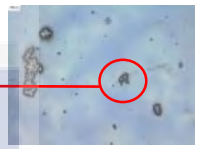
		2		1.506	1.033	
		3		1.116	1.097	
40	60	1	-	0.469	0.561	Dark spot was presumed as AgNPs 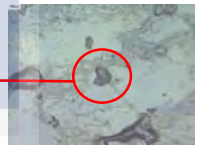
		2		0.228	0.364	
		3		0.340	0.300	
50	50	1	-	0.502	0.245	No obvious colour difference due to the same amount between filler and binder 
		2		0.439	0.240	
		3		1.071	0.383	
60	40	1	136.148	4.238	4.264	Darker colour due to filler amount is higher than binder amount 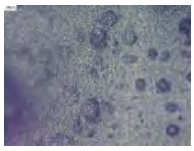
		2	175.222	3.546	4.006	
		3	468.895	3.186	2.319	
70	30	1	40.555	3.516	4.434	Darker colour due to filler amount is higher than binder amount 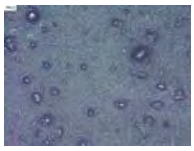
		2	32.080	4.393	3.736	
		3	38.203	4.132	3.257	
80	20	1	6.277	4.335	4.299	Darker colour due to filler amount is higher than binder amount 
		2	5.682	3.366	3.461	
		3	12.927	3.740	2.169	
90	10	1	0.143	4.765	5.721	Obvious colour difference that indicates filler and binder 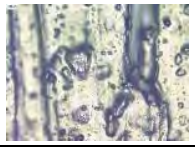
		2	0.100	5.279	5.890	
		3	0.085	5.641	5.716	

In Table 4.27, it exhibited each composition of sample with three parameters; total average values of resistivity, total average values of resistivity and microstructure in order to construct a study of the relationship between sample composition and those three parameters.

For 10% of filler until 50% of filler, there was no resistivity value was detected by four point probe in relations with the filler composition itself that was low. Material of filler was silver nanoparticles which widely known as conductor, so if the amount was low, it was possible that that there was no resistivity being traced.

Furthermore, the total average values of surface roughness were in the range of 0.1 μm up to 1.2 μm and the values of total average values of surface roughness between horizontal direction and vertical direction claimed small difference. The difference indicated of even spreading of ink which made the surface has stable consistency of irregularities. On top of that, the ink being distributed evenly was contributed from the texture of sample that was less concentrated; in low viscosity thus, the printing activity became easier to carry out.

Apart from that, the sample texture that had low viscosity was related to the composition between the elements in the sample which the ratio of binder and hardener was higher than the ratio of filler. Of having more binder and hardener in the sample, their microstructural behaviours was presumed of showing brighter colour of microstructure as they were in transparent form.

Then, from 60% until 90% of filler, the resistivity was detected with 60% having the highest total average value of resistivity, 468.895 Ω/sq and the lowest was 0.1 Ω/sq from 90% of filler yet it had the highest value of conductivity as the resistivity varies inversely with the conductivity value.

Moreover, the total average values of surface roughness were in the range of 2 – 5.9 µm with the highest value was 5.890 µm resulted from 90% of filler and the lowest value was 2.169 µm resulted form 80% of filler both in vertical direction. Being in high total average value of surface roughness, it can be presumed from the ratio of filler was higher that the ratio of binder and hardener and in addition, the filler was in the form of silver flake which strongly made the assumption accepted.

As the sample had high composition of filler, its texture was in high viscosity and became more concentrated, thus during printing process, it required extra work than usual to enable the ink covering the substrate evenly that contributed to the rougher surface. Aside from having rougher surface, more filler in the sample was assumed to generate dotted spot or darker region in the microstructure as the silver nanoparticles were in dark to black colour. In addition, high difference of composition between filler and binder plus hardener was presumed to attribute to the obvious colour difference in microstructure; brighter region versus dark region displayed in 90% of filler.

From all the results from Table 4.27, they attributed that the samples with higher filler percentage had lower resistivity value and increasing value of surface roughness and vice versa. As for the microstructure, it was required in order to make the analysis from those two parameters; resistivity and surface roughness acceptable to find the best print resolution for optimizing the performance of printed electronics.

4.6 SUMMARY

From this chapter, the analysis on the performance of ink categorized based on the filler loading has been conducted through the behaviour of ink. Its behaviour has been characterized through the resistivity, surface roughness and its microstructure of ink.

After the resistivity result obtained, only then one of the objectives can be achieved once ink with the best conductivity has been found out with the help of surface roughness. For the microstructure, it was needed to identify any traces of filler or binder or hardener within the ink.

CHAPTER 5

CONCLUSIONS AND RECOMMENDATION

5.1 INTRODUCTION

From this chapter, a summarized conclusion was described after all of three sections in the flowchart from Chapter 3 has been completed so that the requirement from two objectives will be fulfilled where the relationship between sheet resistivity, surface texture and morphological analysis for silver nanoparticles-filled epoxy conductive ink has been identified.

5.2 CONCLUSIONS

Through the formulation of ink, all of the processes including mixing process, printing process and curing process can be performed to fabricate the ink on the substrates. After the fabrication has been carried out, the behaviour of conductive ink is investigated through the electrical testing, tribological testing and microscopy testing in order to decide the relationship between the results from those three testing in silver nanoparticles-filled epoxy conductive ink.

If the sheet resistivity is subjected, it can be concluded that the filler loading which did not have any presence of conductivity were 10%, 20%, 30%, 40% and 50%, while the filler of loading 60%, 70%, 80% and 90% displayed the presence of conductivity, thus the decision to choose the best filler loading was merely based on

the filler of loading 60%, 70%, 80% and 90% only. Moreover, at filler in the range from 60% until 90% showed a stable adhesion to the substrate.

Otherwise, if the surface texture is the highlight of the subject, it can be summarized from the results of average value of surface roughness; they attributed that the samples with lower filler percentage had consistent average value and smooth surface. Meanwhile, for the samples with high percentage of filler had inconsistent surface irregularities that contributed to rougher surface.

As for the morphological analysis, the microstructure of the sample was needed in order to support the analysis from those two parameters; resistivity and surface roughness so that they will be acceptable to identify the best print resolution for optimizing the performance of printed electronics.

5.3 RECOMMENDATION

Various improvements of conductive ink have been identified through the application of conductive inks in some industries, for example in medical and sports. There are some recommendations that can be made from this project which is from the fabrication process. The fabrication process to produce ink can be improved through the methods of mixing and printing used in this experiment as they should be adjusted to ensure a good result will be obtained. During the mixing process, tolerance of composition of ink loading must be included in consideration to the loss in weight of materials.

For the future works in this project, it is recommended that the conductive ink to be printed on two types of substrates; Polyethylene Terephthalate (PET) and Thermoplastic Polyurethane (TPU) instead of glass substrate. As for the materials involved to produce conductive ink, it is suggested that the materials to be considered are silver powder, silver flake, gold, copper, aluminium and others.

REFERENCES

Ahn, B. Y., Duoss, E. B., Motala, M. J., Guo, X., Park, S. I., Xiong, Y., ... & Lewis, J. A. (2009). Omnidirectional printing of flexible, stretchable, and spanning silver microelectrodes. *Science*, *323*(5921), 1590-1593.

Allen, M. L., Aronniemi, M., Mattila, T., Alastalo, A., Ojanperä, K., Suhonen, M., & Seppä, H. (2008). Electrical sintering of nanoparticle structures. *Nanotechnology*, *19*(17), 175201.

Andersson, H., Manuilskiy, A., Lidenmark, C., Gao, J., Öhlund, T., Forsberg, S., ... & Nilsson, H. E. (2013). The influence of paper coating content on room temperature sintering of silver nanoparticle ink. *Nanotechnology*, *24*(45), 455203.

Bhore, S. S. (2013). Formulation and Evaluation of Resistive Inks for Applications in Printed Electronics.

Bernds, A., Rost, H., & Knobloch, A. (2008). *U.S. Patent No. 7,329,559*. Washington, DC: U.S. Patent and Trademark Office.

Bois, C., Blayo, A., Chaussy, D., Vincent, R., Mercier, A. G., & Nayoze, C. (2012). Catalyst layers for PEMFC manufactured by flexography printing process: performances and structure. *Fuel Cells*, *12*(2), 199-211.

Burton, J. (2008). A primer on UV-Curable Inkjet Inks.

Chan, C. M., Ko, T. M., & Hiraoka, H. (1996). Polymer surface modification by plasmas and photons. *Surface science reports*, *24*(1-2), 1-54.

Chen, S. P., Chiu, H. L., Wang, P. H., & Liao, Y. C. (2015). Inkjet printed conductive tracks for printed electronics. *ECS Journal of Solid State Science and Technology*, *4*(4), P3026-P3033.

Chen, X., Sun, M., & Xiao, F. (2010, August). Preparation of nano silver pastes applied in printed electronics. In *Electronic Packaging Technology & High Density Packaging (ICEPT-HDP), 2010 11th International Conference on* (pp. 279-282). IEEE.

Dang, M. C., Dang, T. M. D., & Fribourg-Blanc, E. (2014). Silver nanoparticles ink synthesis for conductive patterns fabrication using inkjet printing technology. *Advances in Natural Sciences: Nanoscience and Nanotechnology*, *6*(1), 015003.2.5 substrate.

Denneulin, A., Bras, J., Blayo, A., Khelifi, B., Roussel-Dherbey, F., & Neuman, C. (2009). The influence of carbon nanotubes in inkjet printing of conductive polymer suspensions. *Nanotechnology*, *20*(38), 385701.

Dogome, K., Enomae, T., & Isogai, A. (2013). Method for controlling surface energies of paper substrates to create paper-based printed electronics. *Chemical Engineering and Processing: Process Intensification*, *68*, 21-25.

Felba, J., Smolarek, A., Moscicki, A., Falat, T., Zawierta, M., & Zaluk, Z. (2013, September). Improvement of low-temperature sintered ink containing nano-Ag for ink-jet printing of conductive structures on flexible substrates. In *Microelectronics Packaging Conference (EMPC), 2013 European* (pp. 1-6). IEEE.

Felba, J., Nitsch, K., Piasecki, T., Paluch, P., Moscicki, A., & Kinart, A. (2009, July). The influence of thermal process on electrical conductivity of microstructures: Made by ink-jet painting with the use of ink containing nano sized silver particles. In *Nanotechnology, 2009. IEEE-NANO 2009. 9th IEEE Conference on* (pp. 408-411). IEEE.Jiang, S. (2017). Inkjet Printing of Nano-Silver Conductive Ink on PET Substrate.

Gamerith, S., Klug, A., Scheiber, H., Scherf, U., Moderegger, E., & List, E. J. (2007). Direct Ink-Jet Printing of Ag–Cu Nanoparticle and Ag-Precursor Based Electrodes for OFET Applications. *Advanced Functional Materials*, *17*(16), 3111-3118.

Gökkaya, H., & Nalbant, M. (2007). The effects of cutting tool coating on the surface roughness of AISI 1015 steel depending on cutting parameters. *Turkish Journal of Engineering and Environmental Sciences*, *30*(5), 307-316.

Gruner, G. (2007). Carbon nanonets spark new electronics. *Scientific American*, *296*(5), 76-83.

Hrehorova, E., Rebros, M., Pekarovicova, A., Bazuin, B., Ranganathan, A., Garner, S., ... & Boudreau, R. (2011). Gravure printing of conductive inks on glass substrates for applications in printed electronics. *Journal of Display Technology*, *7*(6), 318-324.

Ikeda, O., Watanabe, Y., & Itoh, F. (2007, January). Corrosion measurement of a conductive paste and anisotropic conductive adhesive films. In *Polymers and Adhesives in Microelectronics and Photonics, 2007. Polytronic 2007. 6th International Conference on* (pp. 77-80). IEEE.

Ismail, M., & Jabra, R. (2017). Investigation the parameters affecting on the synthesis of silver nanoparticles by chemical reduction method and printing a conductive pattern, *8*(11), 4152–4159.

Joshi, S. S. (2011). Evaluation of Silver/Graphite Ink Blends for Use in Printed Electronics.

Kamyshny, A., Steinke, J., & Magdassi, S. (2011). Metal-based inkjet inks for printed electronics. *The Open Applied Physics Journal*, *4*(1).

Karwa, A. (2006). Printing studies with conductive inks and exploration of new conducting polymer compositions.

Kazani, I., Hertleer, C., De Mey, G., Schwarz, A., Guxho, G., & Van Langenhove, L. (2012). Electrical conductive textiles obtained by screen printing. *Fibres & Textiles in Eastern Europe*, *20*(1), 57-63.

Kazani, I. (2012). *Study of screen-printed electroconductive textile materials* (Doctoral dissertation, Ghent University).

Kela, L. (2014). Metallic nanoparticles for conductive inks Author (s) Kela, Laura; Auvinen, Ari; Tapper, Unto; Hokkinen, Jouni Citation Int.

Kim, D., Park, J., Jeong, S., & Moon, J. (2005, January). Ink-Jet Printing of Silver Conductive Patterns for Flexible Electronics. In *NIP & Digital Fabrication Conference* (Vol. 2005, No. 3, pp. 93-95). Society for Imaging Science and Technology.

Kim, D., Jeong, S., Moon, J., & Kang, K. (2006). Ink-jet printing of silver conductive tracks on flexible substrates. *Molecular Crystals and Liquid Crystals*, *459*(1), 45-325.

Kim, D., & Moon, J. (2005). Highly conductive ink jet printed films of nanosilver particles for printable electronics. *Electrochemical and Solid-State Letters*, *8*(11), J30-J33.

Kirkor, E. S., Schricker, A. D., & Scheeline, A. (2006). *U.S. Patent No. 7,097,788*. Washington, DC: U.S. Patent and Trademark Office.

Ko, H., Jhin, J., Byun, D., Lee, J., & Park, D. (2005). Copper thin films on PET prepared at ambient temperature by ECR-CVD. *IEEE Transactions on Components and Packaging Technologies*, *28*(4), 781-784.

Ko, S. H., Pan, H., Grigoropoulos, C. P., Luscombe, C. K., Fréchet, J. M., & Poulikakos, D. (2007). All-inkjet-printed flexible electronics fabrication on a polymer substrate by low-temperature high-resolution selective laser sintering of metal nanoparticles. *Nanotechnology*, *18*(34), 345202.

Krebs, F. C. (2009). Fabrication and processing of polymer solar cells: a review of printing and coating techniques. *Solar energy materials and solar cells*, *93*(4), 394-412.

Lee, K. J., Jun, B. H., Kim, T. H., & Joung, J. (2006). Direct synthesis and inkjetting of silver nanocrystals toward printed electronics. *Nanotechnology*, *17*(9), 2424.

Loher, T., Manessis, D., Heinrich, R., Schmied, B., Vanfleteren, J., Debaets, J., ... & Reichl, H. (2006, December). Stretchable electronic systems. In *Electronics Packaging Technology Conference, 2006. EPTC'06. 8th* (pp. 271-276). IEEE.

Lu, K. (2013). Nanoparticulate materials: synthesis, characterization, and processing. Hoboken, NJ: Wiley.

Lupo, D., Clemens, W., Breitung, S., & Hecker, K. (2013). OE-A roadmap for organic and printed electronics. In *Applications of Organic and Printed Electronics* (pp. 1-26). Springer US.

Määttänen, A., Ihalainen, P., Bollström, R., Toivakka, M., & Peltonen, J. (2010). Wetting and print quality study of an inkjet-printed poly (3-hexylthiophene) on pigment coated papers. *Colloids and Surfaces A: Physicochemical and Engineering Aspects*, *367*(1-3), 76-84.

Maissel, L. I., & Glang, R. (1970). Handbook of thin film technology. *New York: McGraw-Hill, 1970, edited by Maissel, Leon I.; Glang, Reinhard*.

Matsuhisa, N., Kaltenbrunner, M., Yokota, T., Jinno, H., Kuribara, K., Sekitani, T., & Someya, T. (2015). Printable elastic conductors with a high conductivity for electronic textile applications. *Nature communications*, *6*.

Merilampi, S., Björninen, T., Haukka, V., Ruuskanen, P., Ukkonen, L., & Sydänheimo, L. (2010). Analysis of electrically conductive silver ink on stretchable substrates under tensile load. *Microelectronics Reliability*, *50*(12), 2001-2011.

Merilampi, S., Laine-Ma, T., & Ruuskanen, P. (2009). The characterization of electrically conductive silver ink patterns on flexible substrates. *Microelectronics reliability*, *49*(7), 782-790.

Moscicki, A., Felba, J., Sobierajski, T., Kudzia, J., Arp, A., & Meyer, W. (2005, October). Electrically conductive formulations filled nano size silver filler for ink-jet technology. In *Polymers and Adhesives in Microelectronics and Photonics, Polytronic, 2005. Polytronic 2005. 5th International Conference on* (pp. 40-44). IEEE.

Nash, C., Spiesschaert, Y., Amarandei, G., Stoeva, Z., Tomov, R. I., Tonchev, D., ... & Glowacki, B. A. (2015). A Comparative Study on the Conductive Properties of Coated and Printed Silver Layers on a Paper Substrate. *Journal of Electronic Materials*, *44*(1), 497.

Nir, M. M., Zamir, D., Haymov, I., Ben-Asher, L., Cohen, O., Faulkner, B., & De La Vega, F. (2010). Electrically conductive inks for inkjet printing. *The Chemistry of Inkjet Inks*, 225-254.

Öhlund, T. (2014). *Metal films for printed electronics: Ink-substrate interactions and sintering* (Doctoral dissertation, Mid Sweden University).

Oldenburg, S. J. (2017). Silver Nanoparticles: Properties and Applications. Retrieved December 12, 2017, from https://www.sigmaaldrich.com/technical-documents/articles/materials-science/nanomaterials/silver-nanoparticles.html

Perelaer, J., De Laat, A. W., Hendriks, C. E., & Schubert, U. S. (2008). Inkjet-printed silver tracks: low temperature curing and thermal stability investigation. *Journal of Materials Chemistry*, *18*(27), 3209-3215.

Reinhold, I., Hendriks, C. E., Eckardt, R., Kranenburg, J. M., Perelaer, J., Baumann, R. R., & Schubert, U. S. (2009). Argon plasma sintering of inkjet printed silver tracks on polymer substrates. *Journal of Materials Chemistry*, *19*(21), 3384-3388.

Roberson, D. A., Wicker, R. B., Murr, L. E., Church, K., & MacDonald, E. (2011). Microstructural and process characterization of conductive traces printed from Ag particulate inks. *Materials*, *4*(6), 963-979.

Samano, A. (2017). *Measurements of conductive film* (Doctoral dissertation, Brunel University London).

Savastano, D. (2015, September 03). Conductive Inks Drive Growth in Flexible and Printed Electronics. Retrieved December 12, 2017, from https://www.printedelectronicsnow.com/issues/2015-03-01/view_features/conductive-inks-drive-growth-in-flexible-and-printed-electronics/

Shen, W., Zhang, X., Huang, Q., Xu, Q., & Song, W. (2014). Preparation of solid silver nanoparticles for inkjet printed flexible electronics with high conductivity. *Nanoscale*, *6*(3), 1622-1628.

Smith, P. J., Shin, D. Y., Stringer, J. E., Derby, B., & Reis, N. (2006). Direct ink-jet printing and low temperature conversion of conductive silver patterns. *Journal of materials science*, *41*(13), 4153-4158.

Smolarek, A., Mościcki, A., Kinart, A., Felba, J., & Falat, T. (2011, May). Dependency of silver nanoparticles protective layers on sintering temperature of printed conductive structures. In *Electronics Technology (ISSE), 2011 34th International Spring Seminar on* (pp. 525-530). IEEE.

Van Osch, T. H., Perelaer, J., de Laat, A. W., & Schubert, U. S. (2008). Inkjet printing of narrow conductive tracks on untreated polymeric substrates. *Advanced Materials*, *20*(2), 343-345.

Wang, Z., Zhao, T., Liang, X., Zhu, P., & Sun, R. (2017, August). A low cost method to synthesize silver nanoparticles for the screen printing conductive inks. In *Electronic Packaging Technology (ICEPT), 2017 18th International Conference on* (pp. 1121-1124). IEEE.

Zheng, G., Cui, Y., Karabulut, E., Wågberg, L., Zhu, H., & Hu, L. (2013). Nanostructured paper for flexible energy and electronic devices. *MRS bulletin*, *38*(4), 320-325.